

dation Flanders (FWO), Belgium, postdoctoral fellowship, PI; Agency for Innovation by Science and Technology-Flanders (IWT), research grant 080020, co-PI; Flemish Government, Belgium, Methusalem excellence grant, key personnel; Belgian Science Policy Office, Interuniversity Attraction Poles program (IUAP) P6/43, key personnel; University of Antwerp, Belgium, Special Research Fund, key personnel; Foundation for Alzheimer Research (SAO-FRMA), Belgium; research grant 09007, PI; Alzheimer's Association, USA, New Investigator Research Grant, NIRG-09-132000, PI; Belgian Parkinson Foundation, Belgium, research grant, PI. L. Bertram, M. Bozi, D. Crosiers, C. Clarke, and M. Facheris report no disclosures. M. Farrer and Mayo Foundation received royalties from H. Lundbeck A/S and Isis Pharmaceuticals. In addition, Dr. Farrer has received an honorarium for a seminar at Genzyme. G. Garraux, S. Gispert, G. Auburger, C. Vilarino-Güell, G.M. Hadjigeorgiou, and A. Hicks report no disclosures. N. Hattori has been serving as an advisory board member for Boehringer Ingelheim; as a result of attending advisory board meetings he received personal compensation. Nobutaka Hattori also has been serving as an advisory board member for FP Pharmaceutical Company by attending these advisory meetings he received personal compensation. He has been consulting with Ohtsuka Pharmaceutical Company, Kyowa Hakko Kirin Pharmaceutical Company, GlaxoSmithKline, Novartis, and Schering-Plough, and when he attended these advisory board meetings, he received personal compensation. B. Jeon has received funding for travel from GlaxoSmithKline Korea and Novartis Korea and has received research support as PI from Novartis, Boehringer Ingelheim, Ipsen Korea, the Korea Health 21 R&D Project, Ministry of Health & Welfare, Republic of Korea (#A030001), ABRC (Advanced Biometric Research Center), KOSEF (Korea Science and Engineering Foundation), Seoul National University Hospital, the Mr. Chung Suk-Gyoo and Singyang Cultural Foundation, and the Song Foundation. S. Lesage, C.M. Lill, and J.-J. Lin report no disclosures. T. Lynch has served on an advisory board for Biogen and Novartis and has received honoraria from Lundbeck, Biogen, and Boehringer-Ingelheim. P. Lichtner reports no disclosures. A.E. Lang has served as an advisor for Abbott, Allon Therapeutics, Astra Zeneca, Biovail, Boehringer-Ingelheim, Cephalon, Ceregene, Eisai, Medtronic, Lundbeck A/S, Novartis, Merck Serono, Solvay, and Teva and received grants from Canadian Institutes of Health Research, Dystonia Medical Research Foundation, Michael J. Fox Foundation, National Parkinson Foundation, and Ontario Problem Gambling Research Centre and has served as an expert witness in cases related to the welding industry. V. Mok reports no disclosures. B. Jasinska-Myga was partially supported by the Robert and Clarice Smith Fellowship Program and the Pacific Alzheimer Research Foundation (PARF) C06-01 grant. G.D. Mellick reports no disclosures. K. E. Morrison has received grant support from Parkinson's UK, The Medical Research Council UK, the Wellcome Trust, and the Midlands Neurological Teaching and Research Fund. G. Opala was partially supported by the Robert and Clarice Smith Fellowship Program and the Pacific Alzheimer Research Foundation (PARF) C06-01 grant. P.P. Pramstaller, I. Pichler, S.S. Park, A. Quattrone, and E. Rogaeva report no disclosures. O.A. Ross is funded by NIH/NINDS awards P50 NS072187 and R01 NS078086, and the Michael J Fox Foundation. L. Stefanis has received a grant for genetic studies of PD from the Hellenic Secretariat of Research and Technology (PENED 2003), in which Novartis Hellas acted as a co-sponsor. J.D. Stockton reports no disclosures. W. Satake receives research support from Japan Intractable Disease Research Foundation. P.A. Silburn and J. Theuns report no disclosures. E.-K. Tan is funded by National Medical Research Council, Duke-NUS Graduate Medical School, and Singapore Millennium Foundation. He has received honoraria from Novartis, Boehringer Ingelheim, and GSK. T. Toda receives research support from Ministry of Health, Labour and Welfare of Japan. H. Tomiyama reports no disclosures. R.J. Uitti has received research funding from the NIH, PARRF, PSG, Noscira, Inc. and Advanced Neuromodulation Systems, Inc. Dr. Uitti has served as a Continuing Medical Educator for the AAN. His institution has received annual royalties from the licensing of the technology related to PARK8/LRRK2 greater than the federal threshold for significant financial interest. Dr. Uitti has not received any royalties. Dr. Uitti receives an honorarium as Associate Editor of *Neurology*<sup>®</sup>. K. Wierdefeldt reports no disclosures. Z. Wszolek holds and has contractual rights for receipt of future royalty payments from patents re: A novel polynucle-

otide involved in heritable Parkinson's disease, receives educational research support from Allergan, Inc., the NIH/NINDS 1RC2NS070276, NS057567, P50NS072187, Mayo Clinic Florida (MCF) Research Committee CR programs (MCF #90052018 and MCF #90052030), and the gift from Carl Edward Bolch, Jr. and Susan Bass Bolch (MCF #90052031/PAU #90052). G. Xiromerisiou, K.-C. Yueh, and Y. Zhao report no disclosures. T. Gasser is funded by Novartis Pharma, the Federal Ministry of Education and Research (BMBF) (NGFN-Plus and ERA-Net NEURON), the Helmholtz Association (HelMA, Helmholtz Alliance for Health in an Ageing Society), and the European Union (MeFoPa, Mendelian Forms of Parkinsonism). He received speaker honoraria from Novartis, Merck-Serono, Schwarz Pharma, Boehringer Ingelheim, and Valeant Pharma and royalties for his consulting activities from Cefalon Pharma and Merck-Serono. Dr. Gasser holds a patent concerning the LRRK2 gene and neurodegenerative disorders. D.M. Maraganore received funding support from the National Institutes of Health grant ES10751 ("Molecular Epidemiology of Parkinson's Disease"). He also received funding support from Alnylam Pharmaceuticals and Medtronic, Inc. to conduct an observational study of Parkinson's disease outcomes. Dr. Maraganore had a patent filed for a method to treat Parkinson disease. It has been licensed to Alnylam Pharmaceuticals. R. Krüger has received research grants of the German Research Council (DFG; KR2119/3-2), the Michael J Fox Foundation, and the Federal Ministry for Education and Research (BMBF, NGFNplus; 01GS08134), as well as speaker honoraria and/or travel grants from UCB Pharma, Cephalon, Abbott Pharmaceuticals, Takeda Pharmaceuticals, and Medtronic. **Go to [Neurology.org](http://Neurology.org) for full disclosures.**

Received July 13, 2011. Accepted in final form January 25, 2012.


## REFERENCES


- Manolio TA, Collins FS, Cox NJ, et al. Finding the missing heritability of complex diseases. *Nature* 2009;461:747-753.
- McCarthy MI, Abecasis GR, Cardon LR, et al. Genome-wide association studies for complex traits: consensus, uncertainty and challenges. *Nat Rev* 2008;9:356-369.
- Simon-Sanchez J, Schulte C, Bras JM, et al. Genome-wide association study reveals genetic risk underlying Parkinson's disease. *Nat Genet* 2009;41:1308-1312.
- Maraganore DM, de Andrade M, Lesnick TG, et al. High-resolution whole-genome association study of Parkinson disease. *Am J Hum Genet* 2005;77:685-693.
- Pankratz N, Wilk JB, Latourelle JC, et al. Genomewide association study for susceptibility genes contributing to familial Parkinson disease. *Hum Genet* 2009;124:593-605.
- Satake W, Nakabayashi Y, Mizuta I, et al. Genome-wide association study identifies common variants at four loci as genetic risk factors for Parkinson's disease. *Nat Genet* 2009;41:1303-1307.
- Saad M, Lesage S, Saint-Pierre A, et al. Genome-wide association study confirms BST1 and suggests a locus on 12q24 as the risk loci for Parkinson's disease in the European population. *Hum Molecul Genet* 20:615-627.
- Spencer CC, Plagnol V, Strange A, et al. Dissection of the genetics of Parkinson's disease identifies an additional association 5' of SNCA and multiple associated haplotypes at 17q21. *Hum Molecul Genet* 20:345-353.
- Hamza TH, Zabetian CP, Tenesa A, et al. Common genetic variation in the HLA region is associated with late-onset sporadic Parkinson's disease. *Nat Genet* 42:781-785.
- Maraganore DM, de Andrade M, Elbaz A, et al. Collaborative analysis of alpha-synuclein gene promoter variability and Parkinson disease. *JAMA* 2006;296:661-670.

11. Simon-Sanchez J, van Hilten JJ, van de Warrenburg B, et al. Genome-wide association study confirms extant PD risk loci among the Dutch. *Eur J Hum Genet* 2011;19:655–661.
12. Mata IF, Yearout D, Alvarez V, et al. Replication of MAPT and SNCA, but not PARK16-18, as susceptibility genes for Parkinson's disease. *Mov Disord* 2011;26:819–823.
13. Simon-Sanchez J, van Hilten JJ, van de Warrenburg B, et al. Genome-wide association study confirms extant PD risk loci among the Dutch. *Eur J Hum Genet* 2011;19:655–661.
14. Nalls MA, Plagnol V, Hernandez DG, et al. Imputation of sequence variants for identification of genetic risks for Parkinson's disease: a meta-analysis of genome-wide association studies. *Lancet* 2011;377:641–649.
15. Ioannidis JP, Thomas G, Daly MJ. Validating, augmenting and refining genome-wide association signals. *Nat Rev* 2009;10:318–329.
16. Higgins JP, Thompson SG. Quantifying heterogeneity in a meta-analysis. *Stat Med* 2002;21:1539–1558.
17. Ioannidis JP, Patsopoulos NA, Evangelou E. Uncertainty in heterogeneity estimates in meta-analyses. *BMJ* 2007;335:914–916.
18. Higgins JP, Thompson SG, Deeks JJ, Altman DG. Measuring inconsistency in meta-analyses. *BMJ* 2003;327:557–560.
19. Clarke GM, Cardon LR. Aspects of observing and claiming allele flips in association studies. *Genet Epidemiol* 2010;34:266–274.
20. Rhodes SL, Sinsheimer JS, Bordelon Y, Bronstein JM, Ritz B. Replication of GWAS associations for GAK and MAPT in Parkinson's disease. *Ann Hum Genet* 2011;75:195–200.
21. Do CB, Tung JY, Dorfman E, et al. Web-based genome-wide association study identifies two novel Loci and a substantial genetic component for Parkinson's disease. *PLoS Genet* 2011;7:e1002141.
22. Nalls MA, Plagnol V, Hernandez DG, et al. Imputation of sequence variants for identification of genetic risks for Parkinson's disease: a meta-analysis of genome-wide association studies. *Lancet* 2011;377:641–649.
23. Ioannidis JP, Patsopoulos NA, Evangelou E. Heterogeneity in meta-analyses of genome-wide association investigations. *PLoS One* 2007;2:e841.
24. Thompson SG. Why sources of heterogeneity in meta-analysis should be investigated. *BMJ* 1994;309:1351–1355.
25. Lewis SJ, Foltynie T, Blackwell AD, Robbins TW, Owen AM, Barker RA. Heterogeneity of Parkinson's disease in the early clinical stages using a data driven approach. *J Neurol Neurosurg Psychiatry* 2005;76:343–348.
26. Wang K, Li M, Hakonarson H. Analysing biological pathways in genome-wide association studies. *Nat Rev Genet* 2010;11:843–854.
27. Fuchs J, Nilsson C, Kachergus J, et al. Phenotypic variation in a large Swedish pedigree due to SNCA duplication and triplication. *Neurology* 2007;68:916–922.
28. Scholz SW, Houlden H, Schulte C, et al. SNCA variants are associated with increased risk for multiple system atrophy. *Ann Neurol* 2009;65:610–614.
29. Zody MC, Jiang Z, Fung HC, et al. Evolutionary toggling of the MAPT 17q21.31 inversion region. *Nat Genet* 2008;40:1076–1083.
30. Ioannidis JP, Ntzani EE, Trikalinos TA. 'Racial' differences in genetic effects for complex diseases. *Nat Genet* 2004;36:1312–1318.

## Visit the *Neurology*<sup>®</sup> Web Site at [www.neurology.org](http://www.neurology.org)

- Enhanced navigation format
- Increased search capability
- Highlighted articles
- Detailed podcast descriptions
- RSS Feeds of current issue and podcasts
- Personal folders for articles and searches
- Mobile device download link
- AAN Web page links
- Links to Neurology Now<sup>®</sup>, Neurology Today<sup>®</sup>, and Continuum<sup>®</sup>
- Resident & Fellow subsite

 Find *Neurology*<sup>®</sup> on Facebook: <http://tinyurl.com/neurologyfan>

 Follow *Neurology*<sup>®</sup> on Twitter: <http://twitter.com/GreenJournal>

# Modeling Alzheimer's Disease with iPSCs Reveals Stress Phenotypes Associated with Intracellular A $\beta$ and Differential Drug Responsiveness

Takayuki Kondo,<sup>1,2,7</sup> Masashi Asai,<sup>7,9,10</sup> Kayoko Tsukita,<sup>1,7</sup> Yumiko Kutoku,<sup>11</sup> Yutaka Ohsawa,<sup>11</sup> Yoshihide Sunada,<sup>11</sup> Keiko Imamura,<sup>1</sup> Naohiro Egawa,<sup>1</sup> Naoki Yahata,<sup>1,7</sup> Keisuke Okita,<sup>1</sup> Kazutoshi Takahashi,<sup>1</sup> Isao Asaka,<sup>1</sup> Takashi Aoi,<sup>1</sup> Akira Watanabe,<sup>1</sup> Kaori Watanabe,<sup>7,10</sup> Chie Kadoya,<sup>7,10</sup> Rie Nakano,<sup>7,10</sup> Dai Watanabe,<sup>3</sup> Kei Maruyama,<sup>9</sup> Osamu Hori,<sup>12</sup> Satoshi Hibino,<sup>13</sup> Tominari Choshi,<sup>13</sup> Tatsutoshi Nakahata,<sup>1</sup> Hiroyuki Hioki,<sup>4</sup> Takeshi Kaneko,<sup>4</sup> Motoko Naitoh,<sup>5</sup> Katsuhiro Yoshikawa,<sup>5</sup> Satoko Yamawaki,<sup>5</sup> Shigehiko Suzuki,<sup>5</sup> Ryuji Hata,<sup>14</sup> Shu-ichi Ueno,<sup>15</sup> Tsuneyoshi Seki,<sup>16</sup> Kazuhiro Kobayashi,<sup>16</sup> Tatsushi Toda,<sup>16</sup> Kazuma Murakami,<sup>6</sup> Kazuhiro Irie,<sup>6</sup> William L. Klein,<sup>17</sup> Hiroshi Mori,<sup>18</sup> Takashi Asada,<sup>19</sup> Ryosuke Takahashi,<sup>2</sup> Nobuhisa Iwata,<sup>7,10,\*</sup> Shinya Yamanaka,<sup>1,8</sup> and Haruhisa Inoue<sup>1,7,8,\*</sup>

<sup>1</sup>Center for iPS Cell Research and Application (CiRA)

<sup>2</sup>Department of Neurology, Graduate School of Medicine

<sup>3</sup>Department of Biological Sciences, Graduate School of Medicine and Department of Molecular and Systems Biology, Graduate School of Biostudies

<sup>4</sup>Department of Morphological Brain Science, Graduate School of Medicine

<sup>5</sup>Department of Plastic and Reconstructive Surgery, Graduate School of Medicine

<sup>6</sup>Organic Chemistry in Life Science, Division of Food Science and Biotechnology, Graduate School of Agriculture Kyoto University, Kyoto 606-8507, Japan

<sup>7</sup>Core Research for Evolutional Science and Technology (CREST)

<sup>8</sup>Yamanaka iPS Cell Special Project

Japan Science and Technology Agency (JST), Saitama 332-0012, Japan

<sup>9</sup>Department of Pharmacology, Faculty of Medicine, Saitama Medical University, Saitama 350-0495, Japan

<sup>10</sup>Laboratory of Molecular Biology and Biotechnology, Department of Molecular Medicinal Sciences, Graduate School of Biomedical Sciences, Nagasaki University, Nagasaki 852-8521, Japan

<sup>11</sup>Department of Neurology, Kawasaki Medical School, Okayama 701-0192, Japan

<sup>12</sup>Department of Neuroanatomy (Biotargeting), Kanazawa University Graduate School of Medical Sciences, Ishikawa 920-8640, Japan

<sup>13</sup>Faculty of Pharmacy and Pharmaceutical Sciences, Fukuyama University, Hiroshima 729-0292, Japan

<sup>14</sup>Department of Functional Histology

<sup>15</sup>Department of Psychiatry

Ehime University Graduate School of Medicine, Ehime 791-0295, Japan

<sup>16</sup>Division of Neurology/Molecular Brain Science, Kobe University Graduate School of Medicine, Kobe, Hyogo 650-0017, Japan

<sup>17</sup>Department of Neurobiology, Northwestern University, Evanston, IL 60208, USA

<sup>18</sup>Department of Neuroscience, Graduate School of Medicine, Osaka City University, Osaka 545-8585, Japan

<sup>19</sup>Department of Neuropsychiatry, Institute of Clinical Medicine, University of Tsukuba, Ibaraki 305-8577, Japan

\*Correspondence: haruhisa@cira.kyoto-u.ac.jp (H.I.), iwata-n@nagasaki-u.ac.jp (N.I.)

<http://dx.doi.org/10.1016/j.stem.2013.01.009>

## SUMMARY

Oligomeric forms of amyloid- $\beta$  peptide (A $\beta$ ) are thought to play a pivotal role in the pathogenesis of Alzheimer's disease (AD), but the mechanism involved is still unclear. Here, we generated induced pluripotent stem cells (iPSCs) from familial and sporadic AD patients and differentiated them into neural cells. A $\beta$  oligomers accumulated in iPSC-derived neurons and astrocytes in cells from patients with a familial amyloid precursor protein (APP)-E693A mutation and sporadic AD, leading to endoplasmic reticulum (ER) and oxidative stress. The accumulated A $\beta$  oligomers were not proteolytically resistant, and docosahexaenoic acid (DHA) treatment alleviated the stress responses in the AD neural cells. Differential manifestation of ER stress and DHA responsiveness may help explain variable clinical

results obtained with the use of DHA treatment and suggests that DHA may in fact be effective for a subset of patients. It also illustrates how patient-specific iPSCs can be useful for analyzing AD pathogenesis and evaluating drugs.

## INTRODUCTION

Alzheimer's disease (AD) is the most prevalent neurodegenerative disorder. One of the pathological features of AD is the oligomerization and aggregation and accumulation of amyloid- $\beta$  peptide (A $\beta$ ), forming amyloid plaques in the brain. Cognitive impairment observed in clinical AD is inversely well correlated with the amount of A $\beta$  oligomers in the soluble fraction rather than the amount of A $\beta$  fibrils (amyloid plaques) constituting the oligomers (Haass and Selkoe, 2007; Krafft and Klein, 2010). Increasing evidence has shown that A $\beta$  oligomers extracted from AD model mice or made from synthetic peptides cause



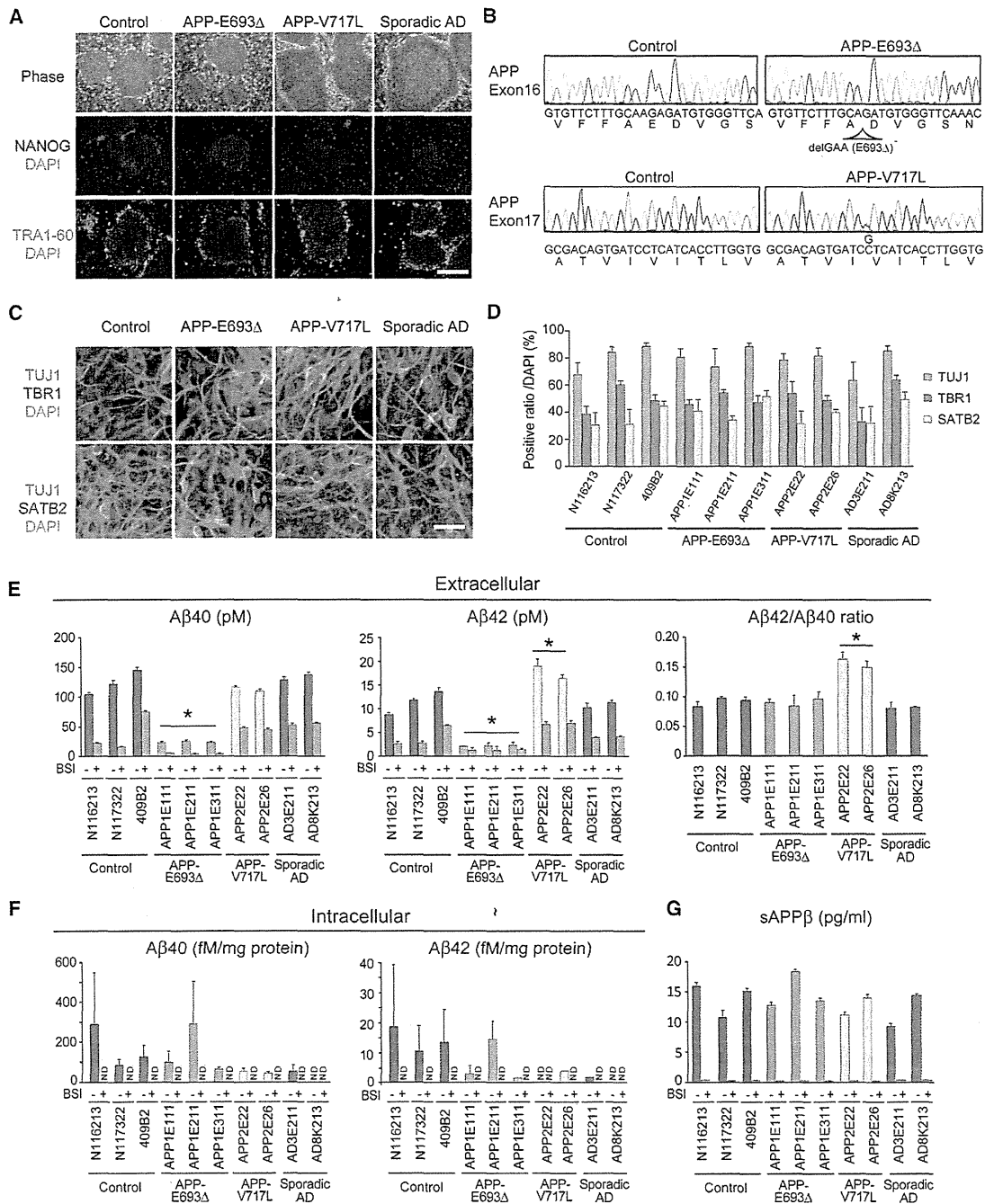


**Figure 1. Establishment of Control and AD Patient-Specific iPSCs, and Derivation of Cortical Neurons Producing Aβs from iPSCs**

(A) Established iPSCs from both controls and AD patients showed embryonic stem cell-like morphology (Phase) and expressed pluripotent stem cell markers NANOG (red) and TRA1-60 (green). The scale bar represents 200 μm.

(B) Genomic DNA sequences showed the presence of the homozygous genotype for E693 deletion and the heterozygous genotype for V717L mutation on the APP gene only in AD iPSCs.

(C) Estimation of neuronal differentiation from control and AD-iPSCs. After 2 months of differentiation, neurons were immunostained with antibodies against the neuronal marker TUJ1 and the cortical neuron markers TBR1 and SATB2. The scale bar represents 30 μm.

(D) Proportions of TUJ1-, TBR1-, and SATB2-positive cells in control and AD-iPSCs. Data represent mean ± SD (n = 3 per clone).

(E) Aβ40 and Aβ42 secreted from iPSC-derived neural cells into the medium (extracellular Aβ) were measured at 48 hr after the last medium change. Data represent mean ± SD (n = 3 per clone). Levels of Aβ40 and Aβ42 in AD(APP-E693Δ) without β-secretase inhibitor IV (BSI, 1 μM) were significantly lower than those of the others (\*, p < 0.006), and the level of Aβ42 and the ratio of Aβ42/Aβ40 in AD(APP-V717L) without BSI were significantly higher than those of the others (legend continued on next page)

neurotoxicity and cognitive impairments in vitro and in vivo (Walsh et al., 2002; Gong et al., 2003; Lesné et al., 2006), and this was also true in humans (Kuo et al., 1996; Shankar et al., 2008; Noguchi et al., 2009). Therefore, the formation and accumulation of A $\beta$  oligomers has been presumed to play a central role in the pathogenesis and clinical symptoms of AD. A $\beta$ s are composed of 38–43 amino acid residues and are generated from the amyloid precursor protein (APP) by  $\beta$ - and  $\gamma$ -secretase-mediated sequential cleavages. A number of mutations linked to familial AD in the *APP* gene have been identified. Recently, an atypical early-onset familial AD, caused by an E693 $\Delta$  mutation of an APP-producing variant A $\beta$  lacking 22<sup>nd</sup> Glu was discovered in Japan (Tomiyama et al., 2008). This APP-E693 $\Delta$  mutation presents rare, autosomal-recessive mutations of the *APP* gene related to familial AD. Patients with the mutation show overt early-onset symptoms of AD but lack A $\beta$  deposition, according to positron emission tomography (PET) scan analysis with a [<sup>11</sup>C] Pittsburgh compound-B (PIB) radioprobe (Tomiyama et al., 2008; Shimada et al., 2011). The 22<sup>nd</sup> Glu within the A $\beta$  sequence has a destabilizing effect on the formation of oligomeric structures because of the electrostatic repulsion between the adjacent side chain of 22<sup>nd</sup> Glu (Kassler et al., 2010), and the deletion of the amino acid residue leads to the ready formation of A $\beta$  oligomers in vitro (Nishitsuji et al., 2009). APP-E693 $\Delta$  transgenic mice show AD-like pathology, including intracellular oligomer accumulation, but lack extracellular amyloid plaque formation (Tomiyama et al., 2010). However, it remains unclear whether A $\beta$  oligomers are accumulated in familial and sporadic AD patient neural cells and how intracellular A $\beta$  oligomers play a pathological role. The compound and/or drugs that might rescue the A $\beta$  oligomer-induced pathological phenotypes are also unclear. Recent developments in induced pluripotent stem cell (iPSC) technology have facilitated the investigation of phenotypes of patient neural cells in vitro and have helped to overcome the lack of success in modeling sporadic AD.

Here, we report the derivation and neuronal and astroglial differentiation of iPSCs from a familial AD patient with an APP-E693 $\Delta$  mutation, a familial case with another APP mutation, as well as other sporadic cases. Using patient neurons and astrocytes, we addressed the accumulation and possible pathological roles of intracellular A $\beta$  oligomers in familial and sporadic AD. We found that A $\beta$  oligomers were not proteolytically resistant and that docosahexaenoic acid (DHA) treatment attenuated cellular phenotypes of AD neural cells with intracellular A $\beta$  oligomers in both familial and sporadic AD patients.

## RESULTS

### iPSC Generation and Cortical-Neuronal Differentiation

Dermal fibroblasts were reprogrammed by episomal vectors (Okita et al., 2011). Control iPSC lines from three unrelated indi-

viduals, three and two familial AD iPSC lines from patients with E693 $\Delta$ [AD(APP-E693 $\Delta$ )] and V717L[AD(APP-V717L)] APP mutations, respectively, and two sporadic iPSC lines (AD3E211 and AD8K213) from two unrelated patients (Figure S1A available online) were generated (Figures 1A, 1B, and S1B–S1H). To characterize cortical neurons derived from the iPSC lines, we established differentiation methods for cortical neurons by modifying previous procedures (Morizane et al., 2011) (Figure S1I). The differentiated cells expressed the cortical neuron subtype markers SATB2 and TBR1 (Figure 1C), and the differentiated neurons were functionally active (Figures S1J and S1K). There was no prominent difference in the differentiation propensity between control and AD neurons (Figures 1D and S1L).

We analyzed the amounts of extra- and intracellular A $\beta$ 40 and A $\beta$ 42 (Figures 1E and 1F). As expected, both A $\beta$  species were strongly decreased in all cloned AD(APP-E693 $\Delta$ ) neural cells in comparison to those in control neural cells. In familial AD(APP-V717L) neural cells, an increase in the extracellular A $\beta$ 42 level and a corresponding decrease in the intracellular A $\beta$ 42 level were observed, and the A $\beta$ 42/A $\beta$ 40 ratio in the culture medium was increased up to 1.5-fold, suggesting that the abnormality of APP metabolism in AD is dependent on the mutation sites in *APP*. Extracellular A $\beta$  levels in sporadic AD neural cells were not changed in comparison to those in control neural cells, but intracellular A $\beta$  in sporadic AD8K213 neural cells apparently decreased (that is, below the detection limit). APP expression levels in the AD(APP-E693 $\Delta$ ) neural cells were lower than in the others, but the levels of  $\alpha$ - and  $\beta$ -secretase-mediated APP processing remained unaltered in all neural cells (Figures 1G, S1M, and S1N). Soluble APP $\beta$  production was strongly inhibited by treatment with  $\beta$ -secretase inhibitor IV (BSI) (Figure 1G). A $\beta$  levels in the original fibroblasts and iPSC-derived astrocytes, in which APP expression levels were relatively higher than those in neural cells (data not shown), were lower than those of the corresponding neural cells (Figures S1O and S1P).

### Intracellular Accumulation of A $\beta$ Oligomers in AD(APP-E693 $\Delta$ ) and in One of the Sporadic AD Neural Cells

Using an immunocytochemical method with the A $\beta$ -oligomer-specific antibody NU1 (Lambert et al., 2007), we investigated whether AD(APP-E693 $\Delta$ ) neural cells harbor A $\beta$  oligomers or not. We found that A $\beta$  oligomers were accumulated as puncta in the neurons of AD(APP-E693 $\Delta$ ) and in one of the sporadic AD cases (Figure 2A). The area of A $\beta$ -oligomer-positive puncta was significantly increased in AD(APP-E693 $\Delta$ ) neuronal cells relative to control neuronal cells (Figure 2B). Dot blot analysis using cell lysates revealed that A $\beta$  oligomers were markedly elevated in the AD(APP-E693 $\Delta$ ) and sporadic AD8K213 neural cells (Figures 2C and 2D), whereas A $\beta$  oligomers were not detected in the culture medium (data not shown). Another antibody against A $\beta$ , 11A1, which detects low-molecular-weight oligomers rather than the A $\beta$  monomer (Murakami et al., 2010), showed results similar to those observed with NU1 (Figures

(\* ,  $p < 0.001$ ). There are significant differences between dimethyl sulfoxide (DMSO)-control and BSI treatment in each case (\* ,  $p < 0.001$ ) except that of AD(APP-E693 $\Delta$ ) for A $\beta$ 42.

(F) A $\beta$ 40 and A $\beta$ 42 in cell lysates (intracellular A $\beta$ ). N.D., not detected. Data represent mean  $\pm$  SD ( $n = 3$  per clone).

(G) The amount of soluble APP $\beta$  was not altered in control and AD. Data represent mean  $\pm$  SD ( $n = 3$  per clone).

See also Figure S1.

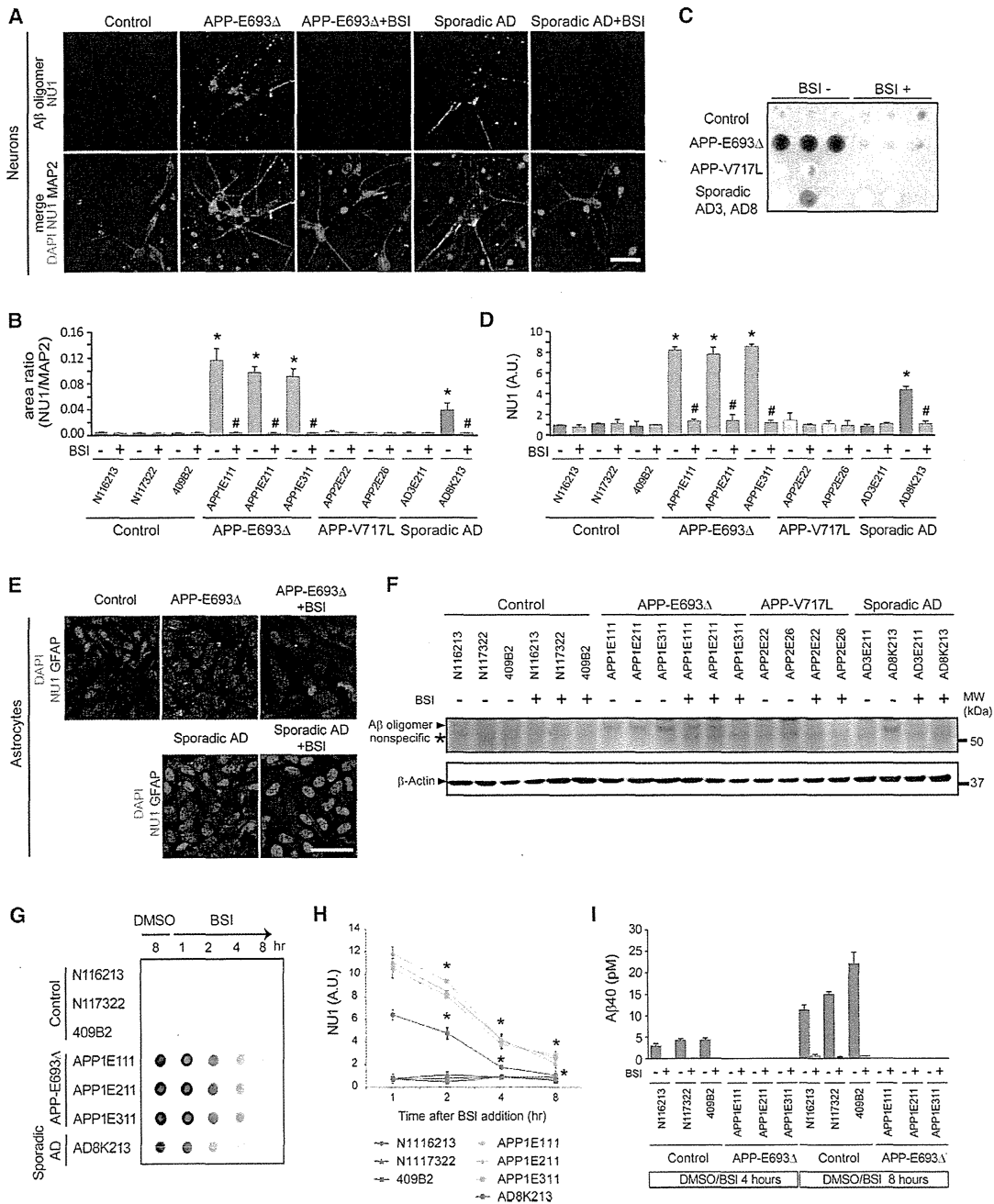


**Figure 2. Familial AD (APP-E693Δ) and Sporadic AD iPSC-Derived Neurons Have Intracellular Aβ Oligomers**

(A) Intracellular Aβ oligomer accumulation in iPSC-derived neurons (red, MAP2-positive cells) was detected by the Aβ-oligomer-specific monoclonal antibody NU1 (green) with a punctate pattern. Aβ oligomer accumulation was massive in AD (APP-E693Δ) and sporadic AD (AD8K213) neurons but only faint in control neurons. Treatment with 1 μM BSI decreased Aβ oligomer accumulation. DAPI, nuclear staining (blue). The scale bar represents 30 μm.

(B) Quantification of Aβ oligomer accumulation in (A); the ratio of the NU1-positive area in the MAP2-positive area was analyzed. Data represent mean ± SD (n = 3 per clone). Aβ oligomer levels in the AD (APP-E693Δ) and sporadic AD (AD8K213) neural cells without BSI were significantly different from those of other neural cells (\*, p < 0.005) and from corresponding neural cells with BSI (#, p < 0.005).

(C) Dot blot analysis with the use of NU1 antibody. Control (N116213, N117322, 409B2), APP-E693Δ (APP1E111, APP1E211, APP1E311), APP-V717L (APP2E22, APP2E26), and sporadic AD (AD3E211, AD8K213) neural cells were dotted from the left. Blank is RIPA buffer only.

(D) Signals of blot in (C) were quantified. Data represent mean ± SD (n = 3 per clone). Aβ oligomer levels in AD (APP-E693Δ) and sporadic AD (AD8K213) neurons without BSI were significantly different from those of other neurons (\*, p < 0.001) and from corresponding neurons treated with 1 μM BSI (#, p < 0.001).

(E) Aβ oligomer accumulation in AD astrocytes. The scale bar represents 30 μm.

(legend continued on next page)

S2A–S2D). However, A $\beta$  oligomers were not detected in cell lysates from the fibroblasts that generate iPSC lines (Figure S2E). To confirm whether A $\beta$  oligomers were derived from mutant APP(E693 $\Delta$ ), we transduced a lentiviral vector driven by an EF1 $\alpha$  promoter to overexpress wild or mutant APP(E693 $\Delta$ ) in control iPSC-derived neural cells and found that A $\beta$  oligomers emerged inside control neural cells overexpressing mutant APP(E693 $\Delta$ ) (Figure S2F).

To investigate the intracellular accumulation of A $\beta$  oligomers in astrocytes derived from control and AD iPSCs, we established an astrocyte-enrichment culture by modifying the method previously reported (Krencik et al., 2011) (Figures S2G–S2J). Dot blot analysis using A $\beta$  oligomer antibodies revealed that the astrocytes of AD(APP-E693 $\Delta$ ) and one of the sporadic AD iPSCs accumulated A $\beta$  oligomers intracellularly (Figures 2E, S2K, and S2L), which was compatible with the results of neurons. On the other hand, we detected no difference in the uptake of extracellular glutamate between control and AD astrocytes (Figure S2M).

A $\beta$  oligomers were also detected as a protein band with a molecular mass of 50–60 kDa by western blot analysis (Figures 2F and S2N). The accumulation of A $\beta$  oligomers was inhibited by treatment with BSI (Figures 2A–2G, S2A–S2D, and S2N). To clarify whether the E693 $\Delta$  mutation results in accelerated A $\beta$  oligomerization and/or in a proteolytically resistant and stable form of A $\beta$  oligomers, we analyzed the levels of A $\beta$  oligomers over a course of time after BSI treatment. Intracellular A $\beta$  oligomers started to disappear from 2 hr after the treatment with BSI, almost reaching the control level by 8 hr (Figures 2G and 2H). Secretion of A $\beta$ 40 from control neural cells was already inhibited at 2 hr after BSI treatment, but the secretion from AD neural cells was under the detection limit in both the presence and absence of BSI (Figure 2I).

#### Cellular Stress Responses Caused By Intracellular A $\beta$ Oligomers in AD iPSC-Derived Neural Cells

Extracellular A $\beta$  deposition in patient brains carrying APP with an E693 $\Delta$  mutation is predicted to be extremely low, as amyloid PET imaging with a [<sup>11</sup>C] PIB probe revealed a far lower signal in the patients than those observed in sporadic AD brains (Tomiya et al., 2008). Given that processing by  $\beta$ - and  $\gamma$ -secretases largely proceeds within vesicular endosomal compartments, it was possible that A $\beta$  oligomers were associated with specific organelles. We characterized the A $\beta$  oligomer-positive punctate structures in AD(APP-E693 $\Delta$ ) neural cells and astrocytes by coimmunostaining with antibodies for markers of vesicular compartments and subcellular organelles. Subpopulations of A $\beta$  oligomer-positive puncta in the AD neurons showed positive immunostaining for an endoplasmic reticulum (ER) marker, binding immunoglobulin protein (BiP); an early endosomal marker, early endosome-associated antigen-1 (EEA1); and

a lysosomal marker, lysosomal-associated marker protein 2 (LAMP2) (data not shown).

To uncover molecules that might be implicated in the dysfunction of AD(APP-E693 $\Delta$ ) neural cells, we analyzed gene expression profiles of control and AD neural cells (Figure 3A and Table S1). Gene ontology analysis revealed that oxidative-stress-related categories, including peroxiredoxin, oxidoreductase, and peroxidase activities, were upregulated in the AD, whereas glycosylation-related categories were downregulated (Figures 3B and 3C and Table S1), suggesting that ER and Golgi function might be perturbed in AD neural cells. Western blot analysis clarified that the amounts of both BiP and cleaved caspase-4 were elevated in the neurons and astrocytes of the AD(APP-E693 $\Delta$ ) case, and that of BiP in one of the sporadic AD cases, AD8K213, but not in fibroblasts (Figures 3D–3F and S3A–S3F). We also found that BSI treatment not only prevented the increase in A $\beta$  oligomer-positive puncta area per cell in the context of AD(APP-E693 $\Delta$ ) lines but also decreased the amount of BiP and cleaved caspase-4 (Figures 3D–3F). *PRDX4*-coding antioxidant protein peroxiredoxin-4 was the most highly upregulated gene (Figure 3C). Western blot analysis confirmed that the amount of peroxiredoxin-4 was increased up to approximately 5- to 7-fold in lysates from AD(APP-E693 $\Delta$ ) and in one of the sporadic AD cases, AD8K213 neural cells, but not in fibroblasts, and was decreased by the BSI treatment (Figures 3D, 3G, S3A, S3D, S3G, and S3H), indicating that the antioxidant stress response was provoked by A $\beta$  oligomer formation in AD(APP-E693 $\Delta$ ) and sporadic AD8K213. To identify pathogenic species evoking oxidative stress in AD(APP-E693 $\Delta$ ), we visualized reactive oxygen species (ROS) and found that ROS was increased in both neurons and astrocytes in AD(APP-E693 $\Delta$ ) and AD8K213 (Figures 3H–3J and S3I–S3L). This increase was counteracted by the BSI treatment. These results indicated that intracellular A $\beta$  oligomers provoked both ER and oxidative stress, and the increase in ROS most likely occurred via a vicious cycle between ER and oxidative stress (Malhotra and Kaufman, 2007).

#### Alleviation of Intracellular A $\beta$ Oligomer-Induced Cellular Stress by DHA

We evaluated BSI and three additional drugs that had been reported to improve ER stress or to inhibit ROS generation: (1) DHA (Begum et al., 2012), (2) dibenzoylmethane (DBM14-26) (Takano et al., 2007), and (3) NSC23766 (Lee et al., 2002) (Figures 4 and S4). DHA treatment significantly decreased the protein level of BiP, cleaved caspase-4, and peroxiredoxin-4 in AD(APP-E693 $\Delta$ ) neural cells (Figures 4A, 4B, S4A, and S4B), and BiP and peroxiredoxin-4 in sporadic AD8K213 (Figures S4C and S4D). Furthermore, DHA treatment also decreased the generation of ROS in AD(APP-E693 $\Delta$ ) neural cells (Figures 4C and 4D), whereas the amount of A $\beta$  oligomers in cell lysates

(F) Western blot analysis of control and AD neural cells in the presence or absence of BSI. BSI treatment (1  $\mu$ M) disappeared 6E10-positive  $\approx$ 55 kDa protein bands in cell lysates of AD(APP-E693 $\Delta$ ) and sporadic AD(AD8K213) neural cells.

(G) Disappearance of A $\beta$  oligomers after BSI treatment was analyzed by dot blot analysis with the use of the NU1 antibody. Intracellular A $\beta$  oligomers started to disappear 2 hr after BSI treatment.

(H) Signals of blots in (G) were quantified. Data represent mean  $\pm$  SD ( $n = 3$  per clone). BSI treatment (1  $\mu$ M) decreased intracellular A $\beta$  in AD neural cells and was reduced to 16–23% of vehicle control by 8 hr. Post hoc analysis revealed that the amounts of A $\beta$  oligomers at 2 hr after BSI treatment were significantly decreased in comparison to those of DMSO control oligomers (\*,  $p < 0.005$ ).

(I) Changes in extracellular A $\beta$ 40 levels were analyzed in the experimental condition of (G). Data represent mean  $\pm$  SD ( $n = 3$  per clone).

See also Figure S2.

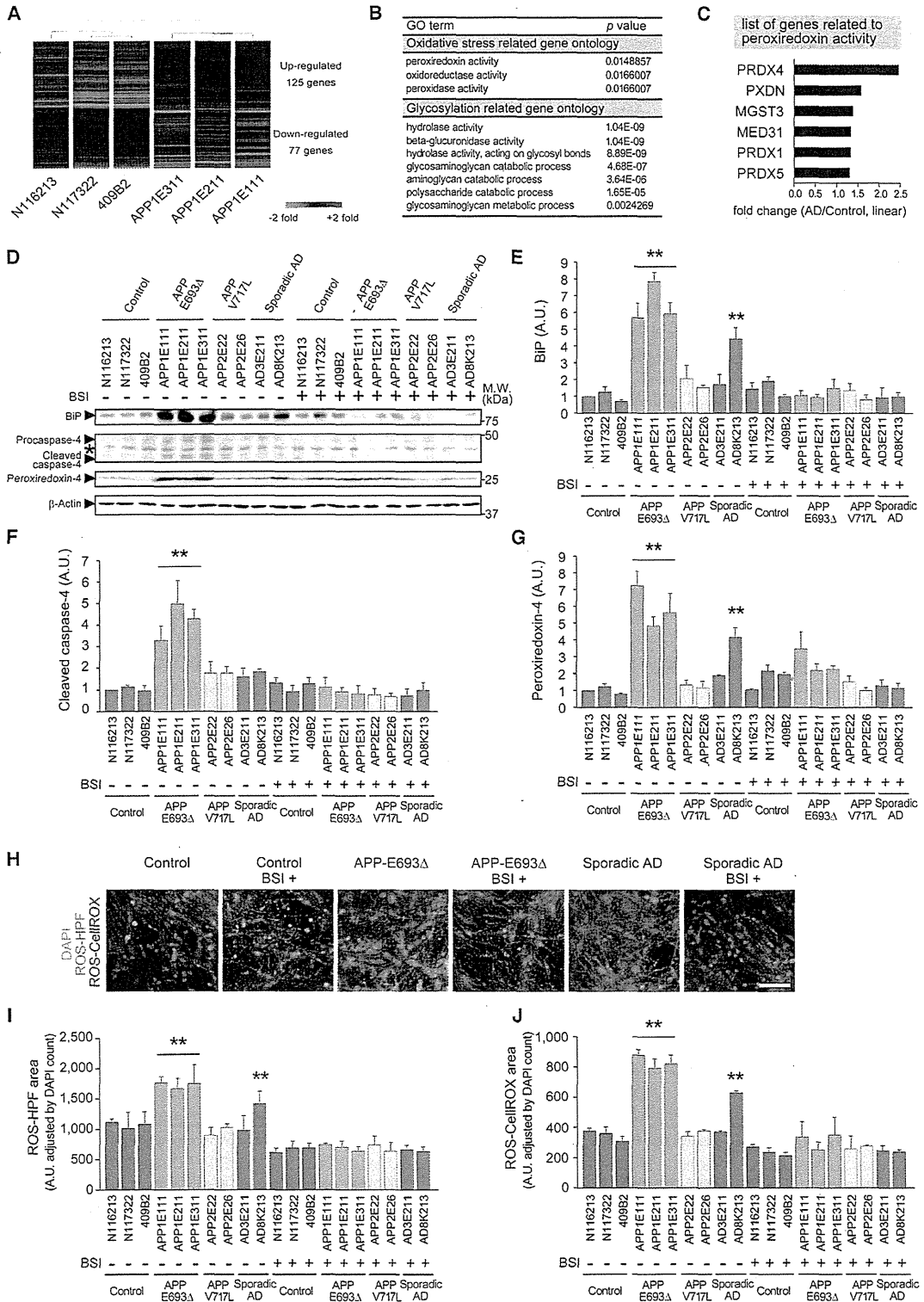


**Figure 3. Cellular Stress Responses Caused by Intracellular A $\beta$  Oligomers in Familial AD (APP-E693 $\Delta$ ) and Sporadic AD (AD8K213) iPSC-Derived Neural Cells**

(A) Hierarchical clustering analysis of differentiated neuronal cells and a heatmap of significantly up- and downregulated genes in AD neural cells. The statistically significant cutoff p value is < 0.05.

(legend continued on next page)



was not altered (Figures S4E–S4G). In contrast, the high concentration of DHA, DBM14-26, or NSC23766 treatment increased the protein level of BiP (Figure S4B). Finally, to confirm the protective effects of DHA in short-term screening, we analyzed the effect on the survival of AD(APP-E693Δ) neural cells. Neuronal cells were labeled with a lentiviral vector expressing synapsin I-promoter-driven EGFP and cultivated in the medium depleted of neurotrophic factors and neural culture supplements mix. The real-time survival rate of AD(APP-E693Δ) neurons was lower than that of normal control neurons; however, DHA treatment for 16 days partially rescued AD(APP-E693Δ) cell viability (Figures 4E–4G). The real-time survival rate of sporadic AD(AD3E211, AD8K213) neurons for 16 days was unchanged (Figures 4E and 4F and Table S2). We confirmed these results through a lactate dehydrogenase (LDH) assay (Figure 4G). The AD(APP-E693Δ) neurons were also vulnerable to oxidative stress by hydrogen peroxide treatment (Figure S4H). Extracellular Aβ levels were not altered in the assay (Figure 4H).

## DISCUSSION

The present study shows that neural cells derived from a patient carrying the pathogenic APP-E693Δ mutation and a sporadic AD patient produce intracellular Aβ oligomers, and the use of these neural cells provided an experimental system for addressing whether such oligomers would cause cellular stress and the killing of neurons and how such intracellular Aβ oligomers might contribute to the disease pathogenesis, despite only one patient carrying the E693Δ mutation being available. Our findings also suggest that the possible heterogeneity of familial and sporadic AD stems from phenotypic differences of intracellular Aβ oligomers and suggests the possibility that DHA, a drug that failed in some clinical trials of AD treatment, might be effective in a portion of AD patients.

We demonstrated that Aβ oligomers were formed and accumulated inside AD(APP-E693Δ) and sporadic AD(AD8K213) neurons by immunostaining (Figures 2A and 2B), dot blot analysis (Figures 2C and 2D), and western blot analysis (Figures 2F and S2N). In addition, intracellular accumulation of Aβ oligomers, which has been supposed to be proteolytically resistant, disappeared after treatment with BSI in both AD neurons (Figures 2G and 2H), indicating that AD(APP-E693Δ) and sporadic AD(AD8K213) neurons still seemed to retain a degrading activity toward Aβ oligomers in which proteasomes, auto-

phagosomes, and/or lysosomes may be involved and, thereby, that the pathological property of Aβ oligomers in a part of AD might be completely abrogated. The sporadic AD(AD8K213) neurons may retain a specific cellular environment that permits the formation of Aβ oligomers. Additional studies aimed at identifying the factors causing such an environment are needed.

We observed that the accumulation of Aβ oligomers induced ER and oxidative stress both in AD(APP-E693Δ) and in sporadic AD(AD8K213) neurons, although caspase-4 activation appeared not to accompany sporadic AD, probably because of the lesser extent of ER stress in comparison to AD(APP-E693Δ). Previously, Nishitsuji et al. (2009) reported that accumulated Aβ oligomers in ER provoke ER stress. This result suggests that oligomers represent a self-aggregating state of Aβ. During this process, Aβ generates ROS, which is supported by the fact that Aβ coordinates the metal ions zinc, iron, and copper, which induce the oligomerization of Aβ. Iron and copper then cause the generation of toxic ROS and calcium dysregulation (Barnham et al., 2004), leading to membrane lipid peroxidation and the impairment of the function of a range of membrane-associated proteins (Hensley et al., 1994; Butterfield, 2003), antioxidant factors being thought to protect ER-stress-induced cellular toxicities (Malhotra and Kaufman, 2007).

We found that intracellular Aβ oligomers were accumulated not only in a case of familial AD with APP-E693Δ mutation but also in a sporadic AD case, although only three clones derived from one familial AD patient carrying an APP-E693Δ mutation and two clones from two sporadic AD patients were analyzed in this study because of the limited number of patients. In contrast, in familial AD with the APP-V717L mutation, of which only one case was available, intracellular Aβ oligomers were not detected, but the extracellular Aβ<sub>42</sub>/Aβ<sub>40</sub> ratio, which is increased in mutant presenilin-mediated familial AD, as reported previously (Yagi et al., 2011), was increased, lending support to the notion that AD could be classified into two categories: extracellular Aβ type and intracellular Aβ type. Although it has been supposed that environmental factors and/or the aging process contribute to neurodegenerative diseases, our findings support the idea that a genetic factor might play a role in a part of sporadic AD, a finding that is compatible with a previous report (Israel et al., 2012). However, identifying the genetic factor would require a larger sample size. The sporadic AD case with intracellular Aβ oligomers might correspond to the case without extracellular Aβ<sub>40</sub> elevation of Israel et al. (2012). Analysis of neurons

(B) The gene ontology (GO) term list, calculated from the significantly altered gene expression patterns in the microarray analysis of AD versus control neural cells.

(C) Altered expression levels of genes related to peroxidation activity detected by GO analysis. All values were significantly different from that of the control ( $p < 0.05$ ).

(D–G) Western blot analysis of ER stress markers (BiP and caspase-4), peroxiredoxin-4, and a reference protein ( $\beta$ -actin) in the presence or absence of BSI.

(E–G) Densitometric analysis of (D) are shown. Measured values of proteins were normalized by  $\beta$ -actin. Data represent mean  $\pm$  SD ( $n = 3$  per clone). Levels of BiP (E), cleaved caspase-4 (F), and peroxiredoxin-4 (G) in AD(APP-E693Δ) and sporadic AD(AD8K213) neural cells without BSI were significantly different from those of the other neural cells (\*\*,  $p < 0.005$ ).

(H) Typical images of reactive oxygen species (ROS) staining, detected by HPF or CellROX, in control and AD neural cells with or without BSI treatment. Scale bars represent 30  $\mu$ m.

(I and J) Quantitative data of (H), ROS-HPF (I), and ROS-CellROX (J). Each value was shown as a ratio of the HPF-stained or CellROX area (average of random 25 fields per sample) adjusted with DAPI counts. Data represent mean  $\pm$  SD ( $n = 3$  per clone). ROS-generation levels in AD(APP-E693Δ) and sporadic AD(AD8K213) neural cells were significantly different from those of the others (\*\*,  $p < 0.001$ ). Data represent mean  $\pm$  SD ( $n = 3$  per clone).

See also Figure S3 and Table S1.

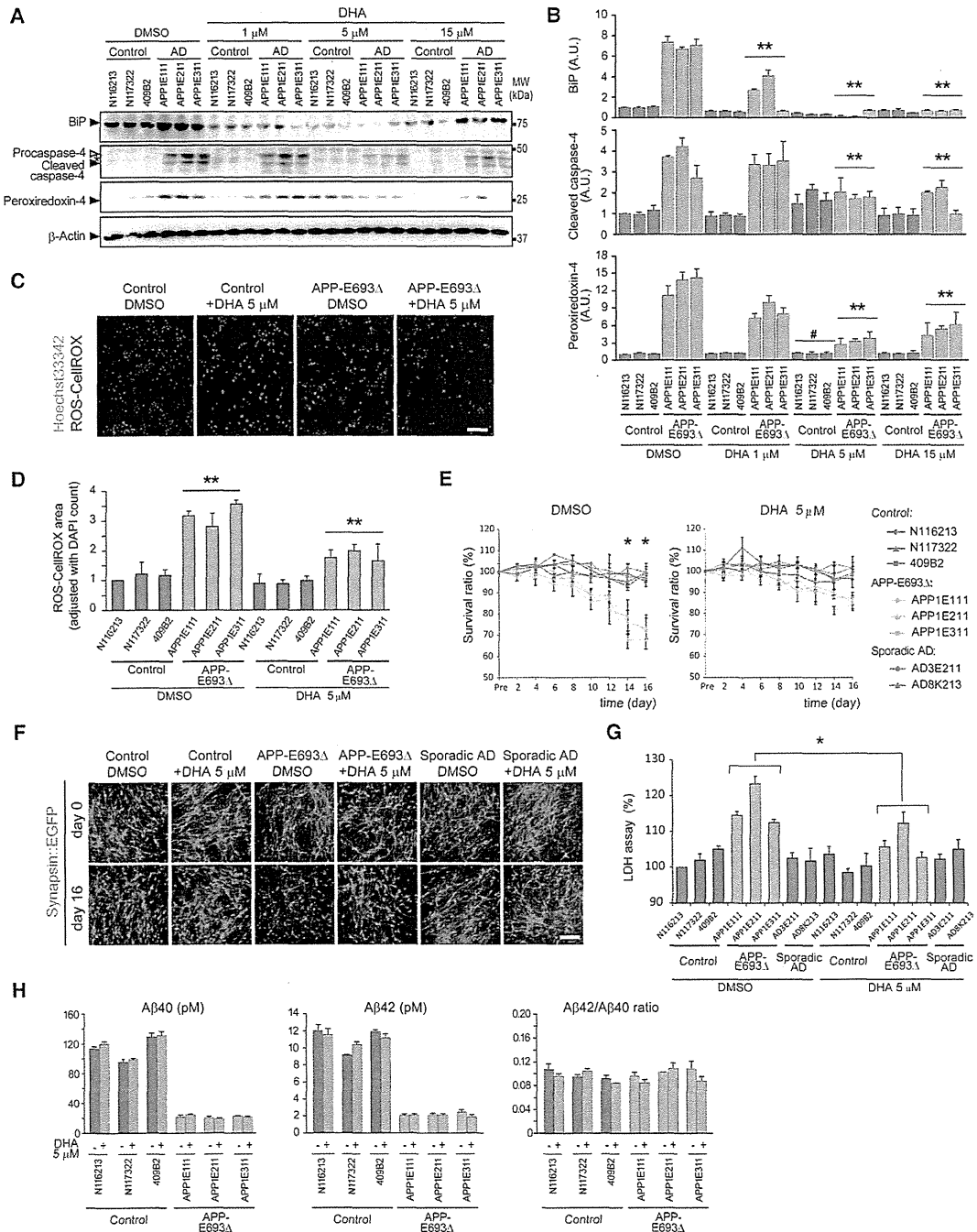


**Figure 4. DHA-Alleviated Cellular Stress Caused By Intracellular A $\beta$  Oligomers**

(A) Control and AD(APP-E693 $\Delta$ ) neural cells at day 72 were treated with DHA for 48 hr. Then, cells were lysed and subjected to immunoblot analysis (1  $\mu$ M, 5  $\mu$ M, and 15  $\mu$ M of docosahexaenoic acid [DHA]).

(B) Densitometric analysis of (A) is shown. Measured values were normalized by that of  $\beta$ -actin. Data represent mean  $\pm$  SD (n = 3 per clone). Two-way analysis of variance (ANOVA) showed significant main effects of DHA treatment (BIP,  $F_{[3,64]} = 136.712$ ,  $p < 0.001$ ; cleaved caspase-4,  $F_{[3,64]} = 50.855$ ,  $p < 0.001$ ) with a significant interaction between APP mutation and DHA treatment (BIP,  $F_{[3,64]} = 99.658$ ,  $p < 0.001$ ; cleaved caspase-4,  $F_{[3,64]} = 53.005$ ,  $p < 0.001$ ). Post hoc analysis revealed significant differences between DMSO (control) and DHA treatment (1, 5, and 15  $\mu$ M) in AD(APP-E693 $\Delta$ ) neural cells (\*\*,  $p < 0.001$ ). Two-way ANOVA for peroxiredoxin-4 showed significant main effects of DHA treatment ( $F_{[3,64]} = 16.995$ ;  $p < 0.001$ ) with a significant interaction between APP mutation and DHA treatment ( $F_{[3,64]} = 32.093$ ;  $p < 0.001$ ). Post hoc analysis revealed significant differences between DMSO-control and DHA treatment (5 and 15  $\mu$ M) in AD(APP-E693 $\Delta$ ) neural cells (\*\*,  $p < 0.001$ ). In control neural cells, the 5  $\mu$ M DHA group was significantly different from the other groups (#,  $p < 0.005$ ).

(C) Typical images of ROS-CeIlROX and Hoechst33342 signals after treatment with vehicle or 5  $\mu$ M DHA. The scale bar represents 50  $\mu$ m.

(legend continued on next page)

and astrocytes, as we performed here, from larger numbers of patients might result in the classification of sporadic AD.

To date, the clinical effectiveness of DHA treatment is still controversial (Freund-Levi et al., 2006; Quinn et al., 2010). It is of particular interest that one of two sporadic AD neurons accumulated intracellular A $\beta$  oligomers and showed cellular phenotypes that could respond to DHA but the other did not, and this result may explain why DHA treatment was effective for some AD patients, those with the intracellular A $\beta$  oligomer-associated type of AD, although the timing (that is, the stage of disease development) for starting the treatment would be another critical factor. These results may suggest that patient-specific iPSCs provide a chance to re-evaluate the effect of a drug that failed in AD clinical trials, depending on the selection of the patient type. In the present study, the amount of A $\beta$  oligomers in our culture was not affected by DHA, although it would be effective for reducing cellular stresses, and reducing the oligomerization of A $\beta$  was also presumed to be a candidate mechanism of DHA treatment (Cole and Frautschy, 2006). These results indicate that therapy with DHA would alleviate symptoms. Furthermore, the data showing that BSI treatment leads to a reduction in ROS formation at a relatively similar level (Figure 2G) in both AD and control cells might indicate an A $\beta$  oligomer-independent effect, in addition to an A $\beta$  oligomer-dependent effect, of BSI.

In any event, patient-specific iPSCs would provide disease pathogenesis, irrespective of the disease being in a familial or sporadic form, as well as enable the evaluation of drug and patient classification of AD.

## EXPERIMENTAL PROCEDURES

### Derivation of Patient-Specific Fibroblasts

Control and AD-derived human dermal fibroblasts (HDFs) were generated from explants of 3 mm dermal biopsies. After 1–2 weeks, fibroblast outgrowths from the explants were passaged.

### iPSC Generation

Human complementary DNAs for reprogramming factors were transduced in HDFs with episomal vectors (*SOX2*, *KLF4*, *OCT4*, *L-MYC*, *LIN28*, and small hairpin RNA for p53). Several days after transduction, fibroblasts were harvested and replated on an SNL feeder cell layer. On the following day, the medium was changed to a primate embryonic stem cell medium (ReproCELL, Japan) supplemented with 4 ng/ml basic FGF (Wako Pure Chemicals Indus-

tries, Japan). The medium was changed every other day. iPSC colonies were picked up 30 days after transduction.

### Statistical Analysis

All data are shown as mean  $\pm$  SD. For comparisons of the mean between two groups, statistical analysis was performed by applying Student's *t* tests after confirming equality between the variances of the groups. When the variances were unequal, Mann-Whitney U tests were performed (SigmaPlot 11.2.0, Systat Software, USA). Comparisons of the mean among three groups or more were performed by one-way, two-way, or three-way analysis of variance followed by a post hoc test with the use of Student-Newman-Keuls Method (SigmaPlot 11.2.0). *p* values < 0.05 were considered significant.

### ACCESSION NUMBERS

The Gene Expression Omnibus accession numbers for microarray data reported in this paper are GSE43326 (gene-expression comparison between control and AD clones), GSE43382 (gene-expression change along with the astroglial differentiation), and GSE43328 (gene-expression comparison of generated iPSCs).

### SUPPLEMENTAL INFORMATION

Supplemental Information contains Supplemental Experimental Procedures, four figures, and two tables and can be found with this article online at <http://dx.doi.org/10.1016/j.stem.2013.01.009>.

### ACKNOWLEDGMENTS

We would like to express our sincere gratitude to all our coworkers and collaborators, Mari Ohnuki, Megumi Kumazaki, Mitsuyo Kawada, Fumihiko Adachi, Takako Enami, and Misato Funayama for technical assistance; Nobuya Inagaki and Norio Harada for technical advice; and Kazumi Murai for editing the manuscript. This research was funded in part by a grant from the Funding Program for World-Leading Innovative R&D on Science and Technology (FIRST Program) of the Japan Society for the Promotion of Science (JSPS) to S.Y., from the Alzheimer's Association (IIRG-09-132098) to H.M., from the JST Yamanaoka iPS Cell Special Project to S.Y. and H.I., from CREST to H.I., H.M., N.I., and T.T., from a Grant-in-Aid from the Ministry of Health, Labour and Welfare of Japan to H.I., from a Grant-in-Aid for Scientific Research on Innovative Area "Foundation of Synapse and Neurocircuit Pathology" (22110007) from the Ministry of Education, Culture, Sports, Science and Technology of Japan to H.I. and N.I., and from the Japan Research Foundation for Clinical Pharmacology to H.I. H.I. conceived the project; T.K., N.I., M.A., and H.I. designed the experiments; T.K., N.I., M.A., K.W., C.K., R.N., N.E., N.Y. and K. Tsukita performed the experiments; T.K., N.I., M.A., and H.I. analyzed the data; K.O., I.A., K.M., T.N., K.I., W.L.K., O.H., S.H., and T.C. contributed

(D) Quantitative data of (C) is shown. Each value indicated the ratio of the CellROX-stained area (an average of random 25 fields per sample) adjusted with DAPI counts. Data represent mean  $\pm$  SD (*n* = 3 per clone). Two-way ANOVA showed significant main effects of DHA treatment ( $F_{[1,32]} = 43.140$ ; *p* < 0.001) with a significant interaction between the APP mutation and DHA treatment ( $F_{[3,32]} = 23.410$ ; *p* < 0.001). The DHA group in AD(APP-E693 $\Delta$ ) neural cells was significantly different from the other groups (\*\*, *p* < 0.005).

(E) Real-time survival rate of control and AD neural cells with and without DHA showing cell viability. The numbers of control and AD(APP-E693 $\Delta$ ) neurons with Synapsin I-promoter-driven EGFP were sequentially imaged (average of 25 random fields per sample) and counted to assess the survival ratio (*n* = 3 per clone). Data represent mean  $\pm$  SD (*n* = 3 per clone). In the cell-survival ratio, three-way ANOVA showed significant main effects of the APP mutation ( $F_{[1,256]} = 377.611$ ; *p* < 0.001), DHA treatment ( $F_{[1,256]} = 36.117$ ; *p* < 0.001), and time ( $F_{[7,256]} = 65.272$ ; *p* < 0.001), with significant interactions between the APP mutation and DHA treatment ( $F_{[1,256]} = 18.315$ ; *p* < 0.001), between the APP mutation and time ( $F_{[7,256]} = 20.023$ ; *p* < 0.001), between DHA treatment and time ( $F_{[7,256]} = 4.534$ ; *p* < 0.001), and among all three factors ( $F_{[7,256]} = 5.277$ ; *p* < 0.001). Post hoc analysis revealed that, on day 14 and day 16, AD(APP-E693 $\Delta$ ) neural cells were more vulnerable in the long culture than control neural cells and that DHA treatment rescued the vulnerability (\*, *p* < 0.001).

(F) Typical images of Synapsin::EGFP neurons used in real-time survival assay. The scale bar represents 50  $\mu$ m.

(G) Cytotoxicity in neural culture derived from control and AD iPSCs after treatment with DHA (5  $\mu$ M) for 16 days. Measured fluorescent lactate dehydrogenase (LDH) release served as a measure of cytotoxicity. Data represent mean  $\pm$  SD (*n* = 3 per clone). Two-way ANOVA showed significant main effects of DHA treatment ( $F_{[1,32]} = 16.710$ ; *p* < 0.001) with a significant interaction between APP-E693 $\Delta$  mutation and DHA treatment ( $F_{[3,32]} = 9.210$ ; *p* < 0.005). There was a significant difference in AD(APP-E693 $\Delta$ ) neural cells between the DMSO-control and DHA groups (\*, *p* < 0.05).

(H) A $\beta$ 40 and A $\beta$ 42 secreted from iPSC-derived neurons into medium (extracellular A $\beta$ ) at day 16 of the long-term culture were measured at 48 hr after the last medium change. Data represent mean  $\pm$  SD (*n* = 3 per clone).

See also Figure S4 and Table S2.

reagents, materials and analysis tools; Y.K., Y.O., Y.S., M.N., K.Y., S.Y., S.S., T.A., R.H., and S.U. recruited the patients; R.T., H.M., and S.Y. provided critical reading and scientific discussions; T.S., K.K., T.T., and K. Takahashi performed microarray analysis; T.A. performed karyotyping; A.W. performed bisulfite genomic sequencing; K.I. and D.W. performed electrophysiology; K. Tsukita, T.K., and H.H. produced the lentivirus; H.I., N.I., M.A., and T.K. wrote the paper. The experimental protocols dealing with human or animal subjects were approved by the institutional review board at each institute. S.Y. is a member without salary of the scientific advisory boards of iPierian, iPS Academia Japan, Megakaryon Corporation, and Retina Institute Japan.

Received: February 27, 2012

Revised: December 22, 2012

Accepted: January 18, 2013

Published: February 21, 2013

## REFERENCES

- Barnham, K.J., Masters, C.L., and Bush, A.I. (2004). Neurodegenerative diseases and oxidative stress. *Nat. Rev. Drug Discov.* **3**, 205–214.
- Begum, G., Kintner, D., Liu, Y., Cramer, S.W., and Sun, D. (2012). DHA inhibits ER  $\text{Ca}^{2+}$  release and ER stress in astrocytes following *in vitro* ischemia. *J. Neurochem.* **120**, 622–630.
- Butterfield, D.A. (2003). Amyloid  $\beta$ -peptide [1–42]-associated free radical-induced oxidative stress and neurodegeneration in Alzheimer's disease brain: mechanisms and consequences. *Curr. Med. Chem.* **10**, 2651–2659.
- Cole, G.M., and Frautschy, S.A. (2006). Docosahexaenoic acid protects from amyloid and dendritic pathology in an Alzheimer's disease mouse model. *Nutr. Health* **18**, 249–259.
- Freund-Levi, Y., Eriksdotter-Jönhagen, M., Cederholm, T., Basun, H., Faxälv, G., Garlind, A., Vedin, I., Vessby, B., Wahlund, L.O., and Palmblad, J. (2006). Omega-3 fatty acid treatment in 174 patients with mild to moderate Alzheimer disease: OmegaAD study: a randomized double-blind trial. *Arch. Neurol.* **63**, 1402–1408.
- Gong, Y., Chang, L., Viola, K.L., Lacor, P.N., Lambert, M.P., Finch, C.E., Krafft, G.A., and Klein, W.L. (2003). Alzheimer's disease-affected brain: presence of oligomeric A  $\beta$  ligands (ADDLs) suggests a molecular basis for reversible memory loss. *Proc. Natl. Acad. Sci. USA* **100**, 10417–10422.
- Haass, C., and Selkoe, D.J. (2007). Soluble protein oligomers in neurodegeneration: lessons from the Alzheimer's amyloid  $\beta$ -peptide. *Nat. Rev. Mol. Cell Biol.* **8**, 101–112.
- Hensley, K., Carney, J.M., Mattson, M.P., Aksenova, M., Harris, M., Wu, J.F., Floyd, R.A., and Butterfield, D.A. (1994). A model for  $\beta$ -amyloid aggregation and neurotoxicity based on free radical generation by the peptide: relevance to Alzheimer disease. *Proc. Natl. Acad. Sci. USA* **91**, 3270–3274.
- Israel, M.A., Yuan, S.H., Bardy, C., Reyna, S.M., Mu, Y., Herrera, C., Hefferan, M.P., Van Gorp, S., Nazor, K.L., Boscolo, F.S., et al. (2012). Probing sporadic and familial Alzheimer's disease using induced pluripotent stem cells. *Nature* **482**, 216–220.
- Kassler, K., Horn, A.H., and Sticht, H. (2010). Effect of pathogenic mutations on the structure and dynamics of Alzheimer's A  $\beta$  42-amyloid oligomers. *J. Mol. Model.* **16**, 1011–1020.
- Krafft, G.A., and Klein, W.L. (2010). ADDLs and the signaling web that leads to Alzheimer's disease. *Neuropharmacology* **59**, 230–242.
- Krencik, R., Weick, J.P., Liu, Y., Zhang, Z.J., and Zhang, S.C. (2011). Specification of transplantable astroglial subtypes from human pluripotent stem cells. *Nat. Biotechnol.* **29**, 528–534.
- Kuo, Y.M., Emmerling, M.R., Vigo-Pelfrey, C., Kasunic, T.C., Kirkpatrick, J.B., Murdoch, G.H., Ball, M.J., and Roher, A.E. (1996). Water-soluble A $\beta$  (N-40, N-42) oligomers in normal and Alzheimer disease brains. *J. Biol. Chem.* **271**, 4077–4081.
- Lambert, M.P., Velasco, P.T., Chang, L., Viola, K.L., Fernandez, S., Lacor, P.N., Khoun, D., Gong, Y., Bigio, E.H., Shaw, P., et al. (2007). Monoclonal antibodies that target pathological assemblies of A $\beta$ . *J. Neurochem.* **100**, 23–35.
- Lee, M., You, H.J., Cho, S.H., Woo, C.H., Yoo, M.H., Joe, E.H., and Kim, J.H. (2002). Implication of the small GTPase Rac1 in the generation of reactive oxygen species in response to  $\beta$ -amyloid in C6 astroglia cells. *Biochem. J.* **366**, 937–943.
- Lesné, S., Koh, M.T., Kotilinek, L., Kaye, R., Glabe, C.G., Yang, A., Gallagher, M., and Ashe, K.H. (2006). A specific amyloid- $\beta$  protein assembly in the brain impairs memory. *Nature* **440**, 352–357.
- Maihotra, J.D., and Kaufman, R.J. (2007). Endoplasmic reticulum stress and oxidative stress: a vicious cycle or a double-edged sword? *Antioxid. Redox Signal.* **9**, 2277–2293.
- Morizane, A., Doi, D., Kikuchi, T., Nishimura, K., and Takahashi, J. (2011). Small-molecule inhibitors of bone morphogenetic protein and activin/nodal signals promote highly efficient neural induction from human pluripotent stem cells. *J. Neurosci. Res.* **89**, 117–126.
- Murakami, K., Horikoshi-Sakuraba, Y., Murata, N., Noda, Y., Masuda, Y., Kinoshita, N., Hatsuta, H., Murayama, S., Shirasawa, T., Shimizu, T., and Irie, K. (2010). Monoclonal antibody against the turn of the 42-residue amyloid  $\beta$ -protein at positions 22 and 23. *ACS Chem. Neurosci.* **1**, 747–756.
- Nishitsuji, K., Tomiyama, T., Ishibashi, K., Ito, K., Teraoka, R., Lambert, M.P., Klein, W.L., and Mori, H. (2009). The E693 $\Delta$  mutation in amyloid precursor protein increases intracellular accumulation of amyloid  $\beta$  oligomers and causes endoplasmic reticulum stress-induced apoptosis in cultured cells. *Am. J. Pathol.* **174**, 957–969.
- Noguchi, A., Matsumura, S., Dezawa, M., Tada, M., Yanazawa, M., Ito, A., Akioka, M., Kikuchi, S., Sato, M., Ideno, S., et al. (2009). Isolation and characterization of patient-derived, toxic, high mass amyloid  $\beta$ -protein (A $\beta$ ) assembly from Alzheimer disease brains. *J. Biol. Chem.* **284**, 32895–32905.
- Okita, K., Matsumura, Y., Sato, Y., Okada, A., Morizane, A., Okamoto, S., Hong, H., Nakagawa, M., Tanabe, K., Tezuka, K., et al. (2011). A more efficient method to generate integration-free human iPS cells. *Nat. Methods* **8**, 409–412.
- Quinn, J.F., Raman, R., Thomas, R.G., Yurko-Mauro, K., Nelson, E.B., Van Dyck, C., Galvin, J.E., Emond, J., Jack, C.R., Jr., Weiner, M., et al. (2010). Docosahexaenoic acid supplementation and cognitive decline in Alzheimer disease: a randomized trial. *JAMA* **304**, 1903–1911.
- Shankar, G.M., Li, S., Mehta, T.H., Garcia-Munoz, A., Shepardson, N.E., Smith, I., Brett, F.M., Farrell, M.A., Rowan, M.J., Lemere, C.A., et al. (2008). Amyloid- $\beta$  protein dimers isolated directly from Alzheimer's brains impair synaptic plasticity and memory. *Nat. Med.* **14**, 837–842.
- Shimada, H., Ataka, S., Tomiyama, T., Takechi, H., Mori, H., and Miki, T. (2011). Clinical course of patients with familial early-onset Alzheimer's disease potentially lacking senile plaques bearing the E693 $\Delta$  mutation in amyloid precursor protein. *Dement. Geriatr. Cogn. Disord.* **32**, 45–54.
- Takano, K., Kitao, Y., Tabata, Y., Miura, H., Sato, K., Takuma, K., Yamada, K., Hibino, S., Choshi, T., Inuma, M., et al. (2007). A dibenzoylmethane derivative protects dopaminergic neurons against both oxidative stress and endoplasmic reticulum stress. *Am. J. Physiol. Cell Physiol.* **293**, C1884–C1894.
- Tomiyama, T., Nagata, T., Shimada, H., Teraoka, R., Fukushima, A., Kanemitsu, H., Takuma, H., Kuwano, R., Imagawa, M., Ataka, S., et al. (2008). A new amyloid  $\beta$  variant favoring oligomerization in Alzheimer's-type dementia. *Ann. Neurol.* **63**, 377–387.
- Tomiyama, T., Matsuyama, S., Iso, H., Umeda, T., Takuma, H., Ohnishi, K., Ishibashi, K., Teraoka, R., Sakama, N., Yamashita, T., et al. (2010). A mouse model of amyloid  $\beta$  oligomers: their contribution to synaptic alteration, abnormal tau phosphorylation, glial activation, and neuronal loss *in vivo*. *J. Neurosci.* **30**, 4845–4856.
- Walsh, D.M., Klyubin, I., Fadeeva, J.V., Cullen, W.K., Anwyl, R., Wolfe, M.S., Rowan, M.J., and Selkoe, D.J. (2002). Naturally secreted oligomers of amyloid  $\beta$  protein potently inhibit hippocampal long-term potentiation *in vivo*. *Nature* **416**, 535–539.
- Yagi, T., Ito, D., Okada, Y., Akamatsu, W., Nihei, Y., Yoshizaki, T., Yamanaka, S., Okano, H., and Suzuki, N. (2011). Modeling familial Alzheimer's disease with induced pluripotent stem cells. *Hum. Mol. Genet.* **20**, 4530–4539.

# Genome-Wide DNA Methylation and Gene Expression Analyses of Monozygotic Twins Discordant for Intelligence Levels

Chih-Chieh Yu<sup>1,9</sup>, Mari Furukawa<sup>1,9</sup>, Kazuhiro Kobayashi<sup>1</sup>, Chizuru Shikishima<sup>2</sup>, Pei-Chieng Cha<sup>1</sup>, Jun Sese<sup>3</sup>, Hiroko Sugawara<sup>4</sup>, Kazuya Iwamoto<sup>5</sup>, Tadafumi Kato<sup>4</sup>, Juko Ando<sup>6</sup>, Tatsushi Toda<sup>1\*</sup>

**1** Division of Neurology/Molecular Brain Science, Kobe University Graduate School of Medicine, Kobe University, Kobe, Japan, **2** Keio Advance Research Centers, Keio University, Tokyo, Japan, **3** Department of Computer Science, Graduate School of Information Science and Engineering, Tokyo Institute of Technology, Tokyo, Japan, **4** Laboratory for Molecular Dynamics of Mental Disorders, RIKEN Brain Science Institute, Saitama, Japan, **5** Department of Molecular Psychiatry, Graduate School of Medicine, The University of Tokyo, Tokyo, Japan, **6** Faculty of Letters, Keio University, Tokyo, Japan

## Abstract

Human intelligence, as measured by intelligence quotient (IQ) tests, demonstrates one of the highest heritabilities among human quantitative traits. Nevertheless, studies to identify quantitative trait loci responsible for intelligence face challenges because of the small effect sizes of individual genes. Phenotypically discordant monozygotic (MZ) twins provide a feasible way to minimize the effects of irrelevant genetic and environmental factors, and should yield more interpretable results by finding epigenetic or gene expression differences between twins. Here we conducted array-based genome-wide DNA methylation and gene expression analyses using 17 pairs of healthy MZ twins discordant intelligently. *ARHGAP18*, related to Rho GTPase, was identified in pair-wise methylation status analysis and validated via direct bisulfite sequencing and quantitative RT-PCR. To perform expression profile analysis, gene set enrichment analysis (GSEA) between the groups of twins with higher IQ and their co-twins revealed up-regulated expression of several ribosome-related genes and DNA replication-related genes in the group with higher IQ. To focus more on individual pairs, we conducted pair-wise GSEA and leading edge analysis, which indicated up-regulated expression of several ion channel-related genes in twins with lower IQ. Our findings implied that these groups of genes may be related to IQ and should shed light on the mechanism underlying human intelligence.

**Citation:** Yu C-C, Furukawa M, Kobayashi K, Shikishima C, Cha P-C, et al. (2012) Genome-Wide DNA Methylation and Gene Expression Analyses of Monozygotic Twins Discordant for Intelligence Levels. PLOS ONE 7(10): e47081. doi:10.1371/journal.pone.0047081

**Editor:** Valerie W. Hu, The George Washington University, United States of America

**Received:** February 9, 2012; **Accepted:** September 11, 2012; **Published:** October 17, 2012

**Copyright:** © 2012 Yu et al. This is an open-access article distributed under the terms of the Creative Commons Attribution License, which permits unrestricted use, distribution, and reproduction in any medium, provided the original author and source are credited.

**Funding:** This work was supported by Grant-in-Aid for Scientific Research on Innovative Areas (22129006 to TT) from the Ministry of Education, Culture, Sports, Science and Technology of Japan; by Grants-in-Aid for Scientific Research (S) (21223002 to JA and TT); by Scientific Research (B) (20390099 to TT); and by Challenging Exploratory Research (23650136 to KK) from the Japan Society for the Promotion of Science. The funders had no role in study design, data collection and analysis, decision to publish, or preparation of the manuscript.

**Competing Interests:** The authors have declared that no competing interests exist.

\* E-mail: toda@med.kobe-u.ac.jp

These authors contributed equally to this work.

## Introduction

Individual differences in cognitive abilities have long been an intriguing phenomenon to both lay people and scientists. Differences in intelligence, as measured by IQ tests, appear to remain relatively stable from childhood to late life [1,2]. Further, the fact that intelligence, in the general population, has a normal distribution and long-term constancy allows for the assumption of the nature of IQ as being, at least partly, hereditary with quantitative trait features. In effect, the heritability of intelligence is estimated to be somewhere between 30% to over 80% in classical MZ twin versus dizygotic twin studies [3–5], marking it one of the highest among human quantitative traits.

Despite the significant role that genes are supposed to play in deciding an individual's cognitive abilities, progress to identify intelligence-related genes in healthy adults is not as promising [6,7], and contrasts the increasing list of some 300 genes associated with mental retardation [8]. One possible explanation for the lack of replicated genetic findings in normal-range intelligence is the

small effect size of each gene. The fact that genome-wide association studies in the scale of thousands of subjects identified no specific genetic variants associated with human intelligence implies that very large sample sizes are necessary to detect individual loci [9].

As underpowered studies face challenges in the attempt to identifying small effect quantitative trait loci, twin research might provide an alternative. Twin studies serve more than a means to estimate heritability of the aforementioned complex traits; they also present an important resource to evaluate quantitative trait loci. There are accumulating evidences that long thought to be genetically identical MZ twins manifest variations in copy number [10] or point mutations limited to one twin [11]; however, these genomic discordances have failed to explain all phenotypic discrepancies [12]. Differences in phenotypes between MZ twins can possibly be attributed to environmental factors, as well as epigenetic variants, which refer to the gene expression-related modifications that occur without altering DNA sequences.

Epigenetic regulatory mechanisms have been reported to be associated with a number of biological phenotypes, including intelligence [13]. Among all known epigenetic mechanisms, DNA methylation has been the most extensively studied. Specifically, such studies have observed patterns of negative correlation between promoter region methylation and gene expression [14]. Additionally, studies based on phenotypically discordant MZ twins have revealed that those who are as best matched for genetics, gender, age, prenatal influences, and shared environment as nature could provide, are considered to possess the potential to detect epigenetic and transcriptomic differences, although research has yet to yield exclusive results [12,15].

In the present study, we recruited 17 healthy MZ twin pairs who manifested discordance for intelligence between co-twins (i.e., more than 1 standard deviation (SD)). Regarding that MZ twins are identical in genetic composition, the IQ difference could be associated with environmental factors, via epigenetic mechanisms regulations. By analyzing array-based genome-wide DNA methylation and gene expression profiles, a novel list of genes with functions related to protein synthesis, DNA helicase activities, and ion channels was generated. To our knowledge, this is the first study tested for epigenetic and expression differences between phenotypically normal, yet discordant, MZ twins via genome-wide approaches.

## Results

### General characteristics of participants

This study is a part of the Keio Twin Study project [16]. We have collected 240 MZ twin pairs with IQ scores of both siblings tested (Fig.S1). Seventeen MZ twin pairs (5 male pairs and 12 female pairs) aged  $25.1 \pm 2.5$  years (range, 21–31 years), with IQ scores of normal range yet manifesting significant between co-twins differences formed the present study sample (Table 1). Mean IQ score of all 34 participants was  $100.91 \pm 13.32$  (range, 67–139), while the mean difference between co-twins was 20.76 points (range, 15–45). No documented psychological or physiological conditions were noted at the time of recruitment. Since there is no standard definition of discordance in MZ twins IQ scores, we adopted 15-point-difference as the principle inclusion criterion. Fifteen-point is not only one standard deviation of IQ scores in general populations, but it is also the average IQ difference for genetically unrelated individuals sharing family environments, whereas identical twins differ by only about 6 IQ points on average [17].

### 27 genes identified by screening for epigenetically regulated candidate loci

We analyzed the methylation profiles of 25,500 human promoters utilizing methylated DNA enriched genomic DNA derived from peripheral blood cells. We used MAT (model-based analysis of tiling arrays) program [18] to identify genes that significantly differed between co-twins pairwisely. With a significance threshold set to  $p < 10^{-6}$ , a total of 27 genes were recognized in 13 of the 17 twin pairs; however, none was shared in plural pairs (Table S1). In addition, a moderate positive correlation of 0.417 (Spearman's rank correlation coefficient,  $p = 0.048$ ) was found between the number of genes that epigenetically differed and pair-wise IQ differences (Fig. S2). On the other hand, after applying the log signal ratio (of the higher IQ twins to the lower IQ co-twins) to one-class *t*-test with the same significance threshold across all 17 twin pairs, we identified no locus manifesting significantly different methylation status.

### Validation of *ARHGAP18* by bisulfite sequencing and quantitative RT-PCR

We performed a sodium bisulfite analysis to confirm the methylation status at the 27 gene loci putatively identified as being differentially methylated. After sequencing at least 30 clones for each locus, statistically significant difference in methylation status between co-twins was validated on two genes, *ARHGAP18* (Rho GTPase activating protein 18,  $p = 5.12806 \times 10^{-8}$ ; chi-square test) and *OR4D10* (olfactory receptor 4D10,  $p = 0.0234658$ ; chi-square test) (Fig. 1A and B).

After confirmation of methylation status, we correlated the data with their expression levels using total RNA derived from lymphoblast cell lines by qRT-PCR. The observed reduction in DNA methylation status of *ARHGAP18* was correlated with its increased expression level in the subject with lower IQ scores of the twin pair from which the gene was identified (2.04 fold,  $p = 0.024767$ ; Mann-Whitney U test) (Fig. 1C, left graph). Increased transcription levels were observed after a 3-day treatment of the demethylating agent 5-aza-2-deoxycytidine (5-aza-dC), and the difference between the twins was eliminated, suggesting that the expression is regulated by the methylation of the promoter (Fig. 1C, right graph). Meanwhile, no expression of *OR4D10* could be detected in the lymphoblast cell lines.

### No gene manifesting statistically significant differences between the group of twins with higher IQ and that of their co-twins after the expression array analysis

Apart from the epigenetic approach described above, we used an expression microarray analysis to directly compare the genome-wide gene expression profiles of the higher IQ twins versus their lower IQ co-twins. At first, principal component analysis (PCA) was performed to facilitate visualization of the relationships between groups (Fig. S3). As a result, the two groups compositing twins with higher or lower IQ scores could not be readily distinguished. Likewise, the dendrograms, produced by hierarchical clustering, also failed to demonstrate differences in general expression patterns between these two phenotypic groups (Fig. S4). Next, ANOVA analysis was applied to identify whether there were differentially expressed genes between these two groups; however, no gene met the criteria of a FDR (false discovery rate)-adjusted  $p$  of 0.05. A one-class *t*-test analysis with multiple sample correction was conducted across all log ratios. Similarly, no significantly differentially expressed gene was identified.

### Candidate genes list resulted from direct pair-wise comparison of the expression array data

Next, we applied a direct pair-wise comparison to focus on the genes up-regulated in the same tendency. Fold-change values of the expression levels of all genes were first calculated for each twin pair, from which genes with a fold-change value more than 2 were included (Dataset S1). We then generated a list of candidate genes by picking up those replicated in most twin pairs (Table 2). *UCHL1* (ubiquitin carboxyl-terminal esterase L1), along with the other 7 genes, were found to have higher expression levels in the higher IQ twins of at least 4 pairs, while 6 genes were up-regulated in some lower IQ twins.

### Identification of 3 genes with borderline significance by grouping samples according to individual gene expression level

To further increase the possibility of identifying candidate genes, we performed an analysis based on individual gene expression level. After dividing the twin siblings of each pair into

**Table 1.** Background data for participants.

Twin Pair ID	Age (year)	Gender	IQ Scores* (Points)		
			Twin A	Twin B	IQ score differences
1	31	F	99	82	17
2	30	F	110	91	19
3	22	M	82	112	-30
4	20	F	100	78	22
5	29	F	90	108	-18
6	20	F	86	104	-18
7	24	F	93	76	17
8	25	F	126	106	20
9	21	M	97	80	17
10	27	F	123	104	19
11	22	F	93	108	-15
12	23	M	97	117	-20
13	27	M	121	139	-18
14	23	M	126	108	18
15	26	F	112	67	45
16	26	F	108	90	18
17	24	F	110	88	22

\*IQ scores calculated after participants took the full version of Kyodai Nx15- test.  
doi:10.1371/journal.pone.0047081.t001

higher and lower expression groups according to the expression level of every gene, a paired t-test was carried out to determine if there was a significant difference between the mean IQ scores of the two groups. Whereas not a single gene reached the corrected cutoff  $p$  of  $10^{-6}$ , 3 genes, *RFK* (riboflavin kinase), *RPL12* (ribosomal protein L12), and *RMRP* (RNA component of mitochondrial RNA processing endoribonuclease), manifested borderline significance (Fig. 2). The twins manifesting up-regulated expression level of *RFK* showed the tendency to have lower IQ scores than their co-twins, while *RPL12* and *RMRP* might likely to contribute to higher intelligence.

#### Identification of 4 differentially expressed gene sets by GSEA

It remained possible that functionally-related genes might have important gene expression changes in a set-wise matter without any individual transcript meeting the criteria of significance. Using GSEA [19] under the cutoff FDR  $q$ -value of  $<0.25$ , we denoted 1 and 4 up-regulated gene sets from KEGG and Gene Ontology (GO) database respectively in the group of higher IQ twins, while 1 gene set each from KEGG and Reactome pathway database was found to be up-regulated in the group of lower IQ twins (Table S2 and Fig. 3). From the results employing GO database, the leading edge analysis revealed 8 genes (*MRPS35*, *MRPL23*, *MRPL52*, *MRPL41*, *MRPL12*, *MRPS15*, *MRPS22*, and *MRPL55*) with core enrichment in the gene sets “Organellar Ribosome,” “Ribosomal Subunit,” and “Mitochondrial Ribosome”, whereas the fourth gene set “ATP-dependent DNA Helicase Activity” was comprised of 7 other genes (*XRCC5*, *XRCC6*, *DHX9*, *PIF1*, *G3BP1*, *RUVBL2*, and *CHDA4*) with core enrichment. By utilizing Reactome database, all 6 genes from the gene set “Reactome CREB phosphorylation through the activation of CAMKII” were enriched.

A different approach was carried out to the same end. Specifically, we performed a GSEA on each twin pair. Depending

on the twin pairs analyzed and pathway databases used, as many as 284 gene sets were found to be significantly different between the siblings (Dataset S2, S3, S4, S5). Gene sets replicated in most twin pairs were listed. In general, pathways related to DNA replication, ribosomes, and proteases were found in higher IQ twins of most twin pairs, while cell signaling associated ones tended to be up-regulated in lower IQ twins (Table 3). In order to focus on those genes which effectively contributed to the enrichment of each given gene set, we first generated up- and down-regulated leading edge subsets for each twin pair, and then extracted those genes that were nominated most often across plural twin pairs (Table 4). Up-regulation of *IGF1* was found in the higher IQ twins of 4 pairs, whereas potassium channel-coding genes *KCNE2* and *KCNQ3*, along with an acetylcholine receptor-coding gene *CHRNA2* manifested higher expression levels in some lower IQ twins. Among all the candidates, *IGF1* was selected for further analysis for its important role in growth and development [20]. We performed bisulfite sequencing of the promoter regions for the 4 twin pairs manifesting an up-regulated expression level in the higher IQ siblings. However, no significant differences were noted in the methylation status of the 2 promoter domains (P1 and P2) between the siblings (Table S3).

#### Discussion

Given that the concept of general cognitive ability, designated as  $g$ , has been widely accepted to depict a near-universal positive covariation among diverse measures of cognitive abilities, naming even one genetic locus that is reliably related with normal-range intelligence remains challenging [21]. IQ is easy to quantify and compare among different individuals. Although not conclusively, the substantial  $g$ -loading for IQ [22] justifies its role to represent the general intelligence levels. Benefiting from the extraordinary similarities in genomic constitution and environmental factors,

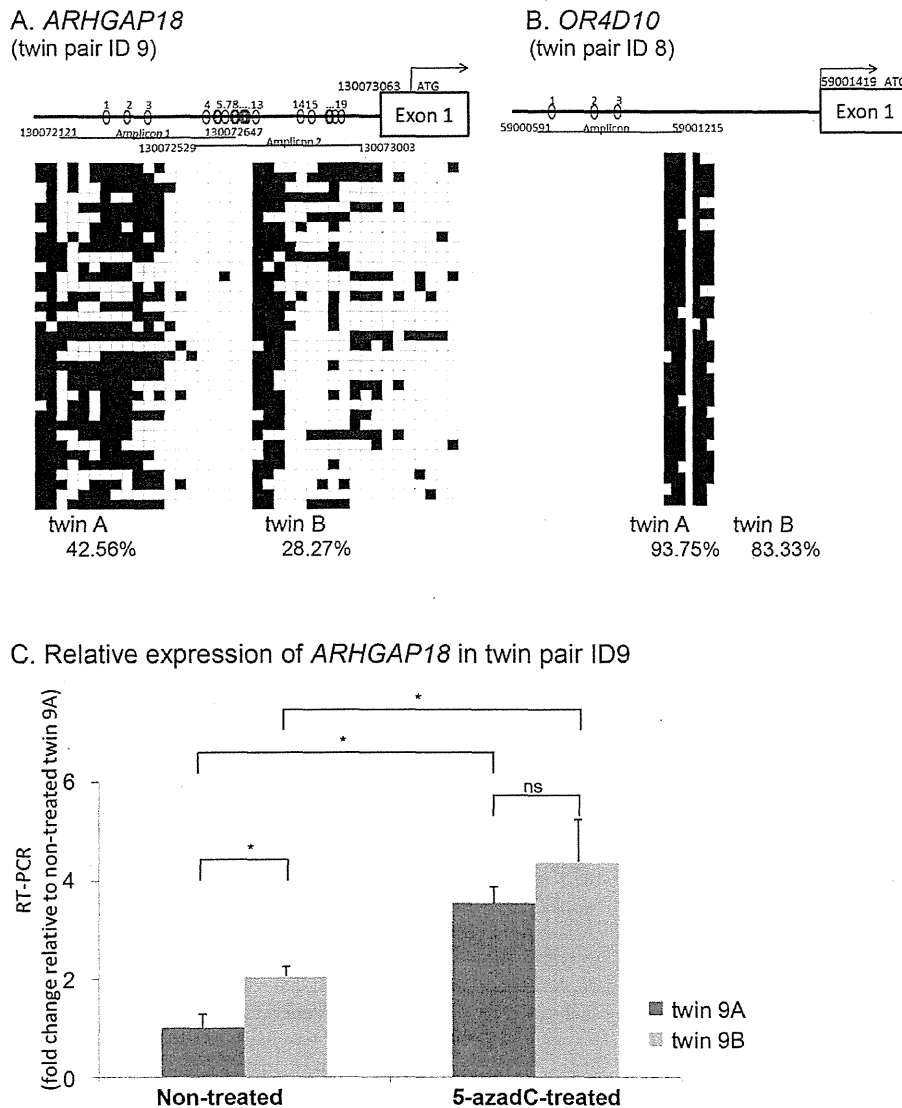


**Figure 1. DNA methylation status of the 5'-regions of *ARHGAP18* and *OR4D10* analyzed by bisulfite sequencing along with the quantitative RT-PCR analysis for *ARHGAP18* expression.** A, B. DNA methylation status analyzed by bisulfite sequencing. Schematic representation (top) for the relative position of CpGs within amplified regions and methylation profiling by bisulfite sequencing (bottom). The numbers at the ends of amplicons indicate the genome coordinates relative to the NCBI Build 36 genome assembly. Of all 27 loci identified by screening for epigenetically regulated candidate genes, A. *ARHGAP18* and B. *OR4D10* were validated by direct bisulfite sequencing. At least 30 clones were sequenced for each locus. Open squares indicate unmethylated CpG nucleotides and closed squares indicate methylated ones. Rows indicate the methylation status of each colony sequenced, while columns indicate the positions of CpG nucleotides. The percentages below refer to the ratio of CpG methylation. C. qRT-PCR analysis of *ARHGAP18* mRNA relative to *GAPDH* in the twin pair ID 9. *ARHGAP18* expression in twin 9A untreated with 5-azadC was normalized to 1. Error bars indicate  $\pm$  SD. *P*-value was calculated using Mann-Whitney U test with asterisks indicating statistical significance ( $p < 0.05$ ). ns: not significant. doi:10.1371/journal.pone.0047081.g001

studies based on discordant monozygotic twins, even with limited sample size (as small as 20–50 twin pairs), are capable of uncovering phenotype-associated epigenetic changes independent of underlying sequence variance [23]. By successfully recruiting 17 pairs of identical twins discordant for intelligence levels, we shall have a modest power in the identification of intelligence-related epigenetic differences. To our knowledge, this is the first genome-wide methylation and gene expression study administering the characteristics of monozygosity to access the epigenetic and expression changes for a quantitative trait.

Researchers have reported that patterns of epigenetic modifications in MZ twins diverge as they age [24]. Provided that all 17 twin pairs in this study were in early adulthood, it might not be surprising that only few loci revealed significant differences in methylation status. Of the 27 candidate loci nominated by promoter-arrays-based methylation analyses, bisulfite sequencing successfully validated only 2 genes. One explanation of the discrepancy between these two methods is that we adopted a less stringent criterion of *p*-value ( $10^{-6}$ , instead of a Bonferroni corrected *p*-value of  $10^{-8}$  considering that GeneChip Human



**Table 2.** List of genes having the same tendency of expression level in most twin pairs.

Up-regulated in co-twins with	Gene	Shared by twin pair ID
Higher IQ scores	<i>GTSF1</i>	1,2,7,11,14,15,16
	<i>AK3L1</i>	1,3,9,11,17
	<i>PRKCH</i>	2,9,11,14,17
	<i>CDRT1</i>	2,9,10,11,14
	<i>LRIG3</i>	1,2,9,15
	<i>VSIG6</i>	2,10,11,13
	<i>SNORA20</i>	3,6,10,12
	<i>UCHL1</i>	8,9,11,15
Lower IQ scores	<i>CD96</i>	1,2,4,9,14
	<i>CXCL10</i>	1,6,9,11
	<i>CDC42BPA</i>	1,2,6,9
	<i>CXCR4</i>	1,2,6,14
	<i>EPS8</i>	2,9,10,16
	<i>FAM169A</i>	3,9,11,15

doi:10.1371/journal.pone.0047081.t002

Promoter 1.0 Array contains 4.6 million probes). As a result, we were able to detect more candidate loci from the practically congruent MZ twin samples, only at the expense of precision rate. The technical limitations of MethylMiner collection might also contribute to false positives. After bisulfite sequencing and qRT-PCR validation, we identified one candidate gene, *ARHGAP18*, which encodes one of the Rho GTPase-activating proteins (GAPs) that modulate cell proliferation, migration, intercellular adhesion, cytokinesis, proliferation differentiation, and apoptosis [25]. Mutations in a handful of Rho-linked genes were documented to

be associated with X-linked mental retardation [8], by which the importance of GAP activity in normal neuronal functions was proposed [26]. Notwithstanding the identification of *ARHGAP18* in a genome-wide association study for schizophrenia [27], it had not been previously connected to cognitive abilities until the present study.

We were not able to identify a single gene that displayed significantly different expression level between the group of twins with higher IQ scores and their co-twins. From the list of candidate genes generated by direct pair-wise comparison, *UCHL1* is a brain-specific de-ubiquitinating enzyme. While the substrates are still unknown, loss of its enzyme activity has been reported in neurological diseases such as Alzheimer's disease and Parkinson's disease [28]. In a different approach, *RFK*, *RPL12*, and *RMRP* showed borderline significance. *RFK* encodes riboflavin kinase, an essential enzyme to form flavin mononucleotide, is important in a wide range of biological metabolisms [29]. *RPL12* encodes a ribosomal protein of the 60S subunit, while *RMRP* encodes the RNA component of mitochondrial RNA processing endoribonuclease. Although none of these 3 genes had ever been connected with cognitive functions, it remains possible that their biophysical characteristics might become more pronounced in cells having as high a metabolic rate as neurons.

In the gene set based approach, GSEA of between-group and between co-twin comparisons revealed several mitochondrial ribosomal protein-coding genes. Mitochondria, which are responsible for most of the energy requirement for cellular metabolism, have their own translation system for the 13 proteins essential for oxidative phosphorylation in mammals. All 78 human mitochondrial ribosome proteins are translation products of nuclear genes, of which some were identified as candidate genes for several congenital diseases [30]. No exclusive conclusion about the connection of mitochondrial ribosomal function and cognitive ability could be drawn before being further validated. Nevertheless, we hypothesized that, for the highly differentiated and high energy-demanding central nervous system, essential proteins for

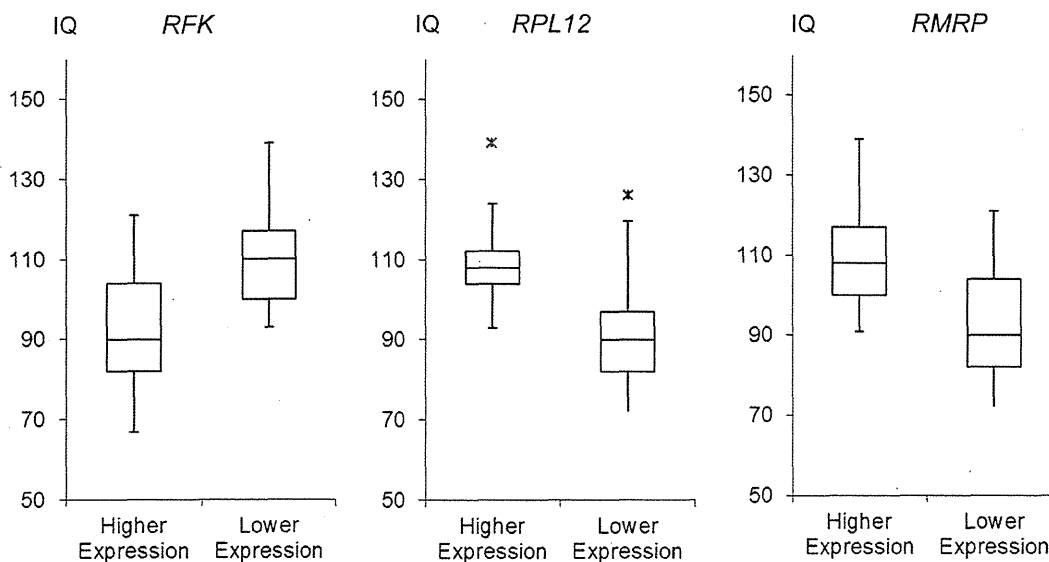


**Figure 2. Three genes manifesting borderline significance by grouping samples according to individual gene expression level.** IQ scores in subjects were grouped according to the relatively higher (Higher Expression) or lower (Lower Expression) expression levels within each twin pair. Three genes, *RFK*, *RPL12*, and *RMRP*, manifested the smallest *p* yet failed to meet the cutoff value of  $p = 10^{-6}$ . Data are presented as box plots (minimum, 25% quartile, median, 75% quartile, maximum). The red asterisks indicate maximum outliers.

doi:10.1371/journal.pone.0047081.g002

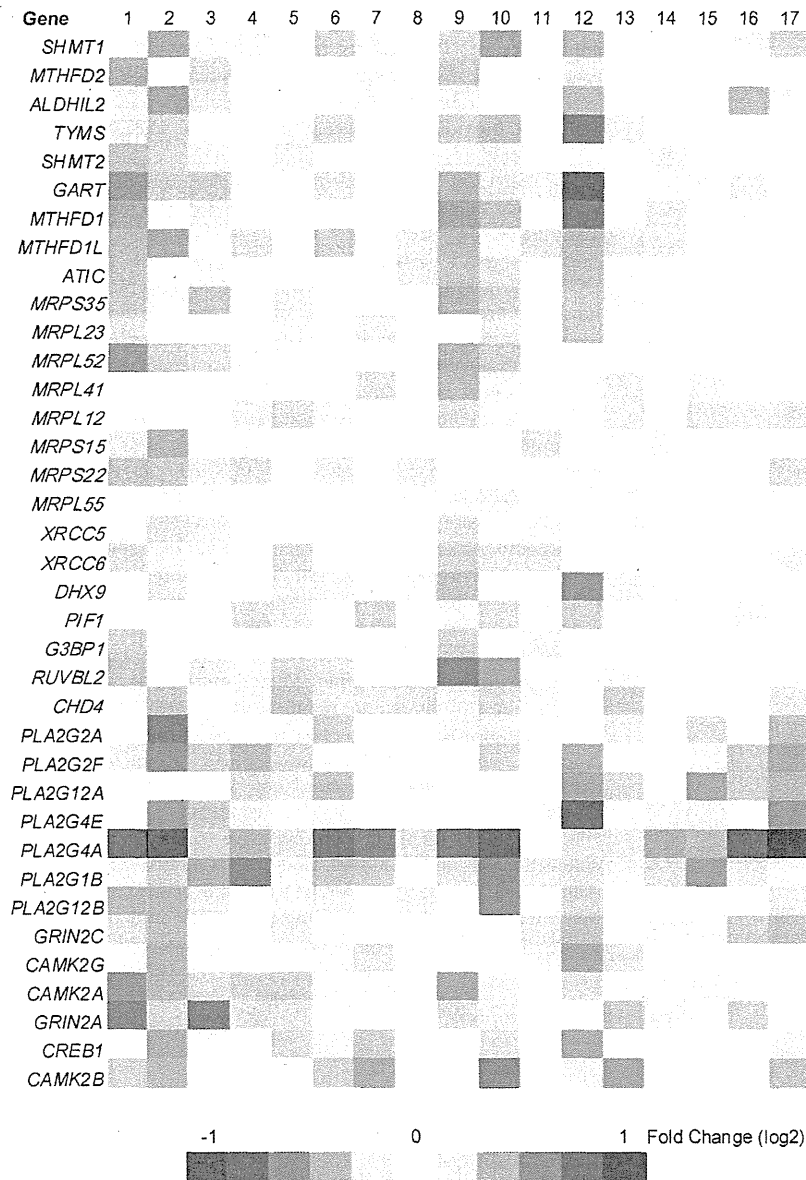


**Figure 3. Heat map of the 37 genes with core enrichment from up-regulated genes sets.** GSEA analysis was carried out to identify if any pre-defined gene set showing different expression levels between the group of higher IQ twins and the group of their lower IQ co-twins. Gene set databases BioCarta, KEGG, Reactome, and Gene Ontology were applied separate. Gene sets meeting the cutoff FDR  $q$ -value of 0.25 were subjected to leading edge analysis to determine the genes with core enrichment. The result was a list of 37 genes and we generated a heat map accordingly. Red and blue cells signify genes that were either up- or down-regulated, respectively, after the expression levels of the twins with higher IQ scores compared to their co-twins. The scale represents fold changes in log<sub>2</sub> values, according to the color map at the bottom of the figure. The general tendency of higher expression levels in twins with higher IQ scores from the gene *SHMT1* to *CHD4*, and their lower expression levels from the gene *PLA2G2A* to *CAMK2B*, was visualized. doi:10.1371/journal.pone.0047081.g003

mitoribosome function might play a role in the maintenance of neuronal biological processes.

Apart from mitochondrial ribosomal protein-related gene sets, “ATP-dependent DNA Helicase Activity” from the GO database was also found. DNA helicases are molecular motor proteins that use nucleoside 5'-triphosphate hydrolysis as a source of energy to open energetically stable duplex DNA into single strands. As such, they are essential in almost all aspects of cellular DNA machinery including DNA replication, repair, recombination, and transcrip-

tion [31]. Of which, *XRCC5* and *XRCC6* encode the two subunits of the Ku protein, which plays an important role in the repair of double-stranded DNA breaks and telomere protection [32]. In neurodegenerative diseases, such as Alzheimer's disease, where cellular damage due to oxidative stress is proposed to contribute to pathophysiology, reduced Ku protein expression and its DNA binding activity have been thought to be involved [33]. Of the remaining five helicases denoted, *G3BP1* was demonstrated to play an essential part in proper embryonic growth and neonatal

**Table 3.** Summary of the most commonly shared gene sets showing the same tendency (up-regulated in the higher IQ twin or in the lower IQ twin) according to the pair-wise GSEA test.

Up-regulated in	Gene sets database	Gene set	Shared by twin pair ID	
Higher IQ twins	BioCarta	MCM pathway	1,9,12,17	
		KEGG	Proteasome	1,3,9,10,17
			Oxidative phosphorylation	1,9,10,12,16
			Ribosome	1,6,9,10,12,16
			DNA replication	1,3,8,9,10,12,17
			Valine leucine and isoleucine degradation	1,3,10,12,17
			Mismatch repair	1,3,9,12,17
			Peroxisome	1,9,10,12,17
		Reactome	RNA polymerase I promoter opening	1,3,9,11,12,13,16,17
			Electrotransport chain	1,3,9,10,12,13,16,17
			Packaging telomere ends	1,3,9,11,12,16,17
			Telomere maintenance	1,3,9,11,12,16,17
		Gene Ontology	Structural constituent of ribosome	9,10,12,17
			Microbody	1,9,12,17
			Peroxisome	1,9,12,17
			S-phase of mitotic cell cycle	1,8,15,17
			Small conjugating protein specific protease activity	1,9,15,17
Lower IQ twins	BioCarta	n/a	n/a	
	KEGG	Neuroactive ligand receptor interaction	1,3,16,17	
		Taste transduction	1,3,9,13,17	
	Reactome	Cell-cell adhesion systems	1,3,9,17	
	Gene Ontology	Anion transport	1,5,16,17	
		Cation channel activity	1,9,16,17	
		Cell-cell signaling	1,9,16,17	
		Collagen	1,9,16,17	
		Extracellular matrix part	1,9,16,17	
		Extracellular region part	1,9,16,17	
		G-protein coupled receptor protein signaling pathway	1,9,16,17	
		Gated channel activity	1,9,16,17	
		Intercellular junction	6,9,16,17	
		Metal ion transmembrane transporter activity	1,9,16,17	
		Second messenger mediated signal	1,9,16,17	

n/a indicates no gene set was shared by at least 4 twin pairs.  
doi:10.1371/journal.pone.0047081.t003

survival [34]. Although the direct associations between these seven genes and cognitive abilities have not been depicted, mutations in a list of DNA repair-related genes have already been reported to cause mental retardation [8]. As such, one hypothesis we proposed here is that the up-regulated expression of these helicases might provide better protection from oxidative damages and, thus, improve neuronal function and survival, which could bring forth higher levels of intelligence (or in other words, less compromised) as a phenotype.

On the other hand, the pair-wise GSEA, along with leading edge analysis, identified *CHRNA2* which encodes the  $\alpha 2$  subunit of nicotinic acetylcholine receptors (nAChRs). Initially related to nicotine dependence, the role of nAChRs in cognitive performance has gained attention because nicotine is considered a powerful enhancer of cognitive capabilities [35] via the interaction of nicotine and nAChRs [36].

Additionally, two potassium voltage-gated channel-coding genes, *KCNE2* and *KCNQ3*, were identified. Voltage-gated ion channels possess diverse functions, include regulating neurotransmitter release, heart rate, insulin secretion, neuronal excitability, epithelial electrolyte transport, and smooth muscle contraction. By assembling with *KCNQ2* or *KCNQ5*, *KCNQ3* forms the M channel, a slow activating and deactivating potassium channel that plays a critical role in the regulation of neuronal excitability [37]. In addition to being identified as one cause for a dominantly inherited form of human generalized epilepsy, called benign familial neonatal convulsions, the electrogenic characteristics of *KCNQ/M* channels have importance in controlling intrinsic firing patterns of principal hippocampal neurons, thus, further modulating hippocampal learning and memory [38]. Of note, rats treated with Linopirdine, an M channel-specific inhibitor,

**Table 4.** Up-regulated genes with core enrichment shared by co-twins of multiple pairs.

Up-regulated in	Gene Sets database	Gene	Shared by twin pair ID		
Higher IQ twins	BioCarta	<i>CASP6</i>	1,10,12,17		
		<i>CCNE1</i>	1,9,12,17		
		<i>IGF1</i>	1,2,7,17		
		<i>IL1a</i>	2,7,8,15		
		<i>LTA</i>	2,8,15,17		
		<i>C7</i>	2,3,8,15		
		<i>IL6</i>	2,3,7,15		
		<i>STAT4</i>	3,8,10,17		
		KEGG	<i>MOM6</i>	1,3,8,9,12,17	
			<i>RPA2</i>	1,3,8,9,12,17	
			<i>POLA2</i>	1,3,8,9,12	
			<i>PRIM2</i>	1,3,8,9,12	
			<i>MOM2</i>	1,3,8,9,12	
			<i>LTA</i>	2,3,10,15,16	
	<i>SDHB</i>		1,3,9,10,16		
	<i>POLE2</i>		1,3,8,9,17		
	<i>COX7C</i>		1,9,10,12,16		
	<i>COX8A</i>		1,9,10,12,16		
	<i>NDUFB7</i>		1,9,10,12,16		
	<i>NDUFA8</i>		1,9,10,12,16		
	<i>NDUFA7</i>		1,9,10,12,16		
	<i>SSBP1</i>	1,8,9,12,17			
	Reactome	<i>NUP93</i>	1,3,9,10,11,12,17		
		<i>POLE2</i>	1,3,9,11,16,17		
		<i>POLR2L</i>	1,3,9,11,12,16		
		<i>POLR2G</i>	1,3,9,12,16,17		
		<i>PSMD14</i>	1,3,9,11,12,17		
		<i>PSMC6</i>	1,3,9,11,12,17		
		<i>RPA2</i>	1,3,9,11,12,17		
		<i>NUP85</i>	1,3,9,10,11,12		
		<i>NUP37</i>	1,3,9,11,12,17		
		<i>NUP205</i>	1,3,9,11,12,17		
	Gene Ontology	n/a	n/a		
		n/a	n/a		
		Lower IQ Twins	KEGG	<i>EP300</i>	1,3,6,12,13
				<i>ACTN1</i>	1,6,12,13,14
				<i>PLOB2</i>	1,3,8,13
				<i>PIK30G</i>	1,6,8,13
				<i>CREBBP</i>	1,3,12,13
	<i>MAPK9</i>			1,2,6,13	
	<i>LEF1</i>			1,3,6,12	
	<i>PIK3R3</i>	2,6,8,13			
	<i>AKR104</i>	3,8,10,17			

**Table 4.** Cont.

Up-regulated in	Gene Sets database	Gene	Shared by twin pair ID
	Reactome	<i>PARD3</i>	6,8,12,16
		<i>MNAT1</i>	2,6,7,14
		<i>RFC2</i>	2,6,7,14
		<i>PRIM1</i>	2,6,7,14
		<i>PRIM2</i>	2,6,7,14
	Gene Ontology	<i>CHRNA2</i>	1,9,16,17
		<i>KCNE2</i>	1,9,16,17
		<i>KCNQ3</i>	1,9,16,17
		<i>INHBA</i>	1,9,14,17
		<i>SLC34A3</i>	1,5,16,17

n/a, no gene was shared by at least 4 twin pairs.  
doi:10.1371/journal.pone.0047081.t004

demonstrated improved performance in various tests of learning and memory [39].

Identified by utilizing BioCarta pathway database, *IGF1* manifested up-regulation in higher IQ twins. The insulin-like growth factor (IGF) system is important in growth and development. While the exact mechanism remains unknown, the growth hormone (GH) and IGF-1 axis has been reported to play a role in the reduction of cognitive functions in aging population and patients with GH deficiency [20]. Methylation status of its promoter regions was studied, yet no difference was discerned between the twins. It is possible that *IGF1* is under some other epigenetic regulation, considering the actual mechanisms responsible for the cell type-specific expression patterns of this gene remain to be elucidated [40].

Since intelligence is a complex trait associated with many genes of small effect [41,42], it was not surprising that we failed to identify a single gene manifesting prevailing expression changes across all 17 twin pairs. We also noticed that by microarrays none of the candidate genes identified by methylation analyses was listed in the results of expression studies. A reason of the discrepancy of these two methods may be the lack of comprehensive accession to all known epigenetic regulations. DNA methylation at CpG sites across promoter regions has been deeply studied, while a number of other epigenetic regulatory mechanisms are also found to modulate gene expression [22]. Furthermore, ever since the genome-wide, single-base human DNA methylome mapping became possible, the correlation of methylation status of gene bodies and expression levels has been gaining attention [43]. It has been documented that DNA methylation of gene bodies is associated with gene activity. Therefore, it is possible that the intelligence-related expression profiles were subjected to this novel epigenetic regulation.

The present study has its conceptual and technical limitations. Conceptually, we hypothesized that changes in methylation status and expression levels could be captured in genomic DNA and total RNA extracted from whole blood and derivative lymphoblastic cell lines, respectively. Given the inability to probe DNA methylation status or gene expression in the human brain, except in postmortem studies, human blood is commonly used in transcriptional studies of various diseases including psychiatric disorders [44]. Although there is still no consensus regarding blood-based gene expression profiles as good surrogates for addressing neuroscientific research, the moderate correlation